10-23-1985

Forecasting for Local Water Management

Douglas Alan Putnam
Portland State University

AN ABSTRACT OF THE THESIS OF Douglas Alan Putman for the Master of Science in Engineering: Civil presented October 23, 1985.

Title: Forecasting For Local Water Management

APPROVED BY MEMBERS OF THE THESIS COMMITTEE

[redacted]

Roy W. Koch, Chairman

[redacted]

Vernon C. Bissell

[redacted]

M. M. Gorji

[redacted]

C. William Savery

Forecast models are investigated and developed for use in local water management to aid in determining short term water requirements and availability. The forecast models include precipitation occurrence

and depth using a Markov chain model, temperature and solar radiation with a multivariate autoregressive model, and streamflow with autoregressive-moving average models. The precipitation, temperature, and solar radiation forecasts are used with a soil moisture model to determine water demands. A state space approach to the Muskingum-Cunge streamflow routing technique is developed. The forecast water demands and streamflow forecasts are used as inputs to this routing model. Forecast model errors and propagation of these errors from one model into the next are investigated.

The models are tested using data from the Tualatin River Basin in Oregon. The results tend to indicate that these models are sufficiently accurate to aid in water management.

FORECASTING FOR LOCAL WATER MANAGEMENT

by

DOUGLAS ALAN PUTMAN

A thesis submitted in partial fulfillment of the requirements for the degree of

MASTER OF SCIENCE
in
ENGINEERING: CIVIL

Portland State University

1985

TO THE OFFICE OF GRADUATE STUDIES AND RESEARCH

The members of the Committee approve the thesis of Douglas Alan Putman presented October 23, 1985

[redacted]

Roy W. Koch, Chairman

[redacted]

Vernon C. Bissell

[redacted]

M. M. Gorji

[redacted]

C. William Savery

APPROVED:

[redacted]

Franz N. Rad, Head, Department of Civil Engineering

[redacted]

Jim F. Heath, Dean of Graduate Studies and Research

ACKNOWLEDGEMENTS

I would like to thank Dr. Roy Koch for his guidance, assistance, and support on this project.

I would also like to thank the Oregon Water Resources Research Institute for providing funding for this project.

TABLE OF CONTENTS

LIST OF TABLES

LIST OF FIGURES

FIGURE PAGE

CHAPTER I

INTRODUCTION

As the need for water continues to increase so does the need to develop methods by which it can be used more wisely. In many regions of the world and even this country, serious water shortages have occurred and will undoubtedly continue to occur in the future. There are several ways in which water supply can be enhanced to attempt to meet demand. In the past the most common solution has been to build structures either for storing water when it is plentiful until the time of need, to build complex transmission systems to get water to where it is needed, or both. Unfortunately, much of this type of construction and development is becoming prohibitively expensive particularly as federal participation decreases. In many parts of the country much of the easily available water has been developed and in the case of groundwater, depleted. More recently, conservation practices have emerged as an alternative to structural development and are being used in industry, agriculture, and even by the individual. At present, mathematical models are being developed so that managers are able to get the "best use" out of the available water resources by predicting the supply and demand of water for use in system operation. Using such models allows the manager to make more informed decisions and provides the ability to optimize water use

even in the time of water shortage. With computers many such tasks that were once far too costly are rapidly becoming an inexpensive way of maximizing the available supply, thus making this approach to water management increasingly popular.

In the Western United States, irrigated agriculture accounts for by far the largest consumptive use of water. Due to the nature of this application, conflicts due to shortages of supply often result among irrigation users, particularly where there is no storage within the system as is often the case in smaller river basins. In addition, considerable attention is now being given to the instream value of water to maintain or enhance water quality and provide for aquatic habitat. These latter uses, by their very nature, conflict with diversion and consumptive use of water for irrigation. Since the distribution of water resources in the West is largely governed by the appropriative doctrine and most of the attention to instream use is relatively recent, any water rights attached to this type of use is junior to the older irrigation rights by the "first in time, first in right" principle.

Although development of additional storage may be an alternative to mitigation of these conflicts, another option is the more efficient use of the resource. For irrigated agriculture, this generally implies more attention to the timing and amount of irrigation water, which in turn requires either measurement or prediction of soil moisture. Since any extensive measurement schemes are labor intensive and thus resonably costly, accurate modeling of the process is an attractive alternative. In addition, the distribution of flow

in the river system is required to estimate availability for future supply. Where storage exists, such information can aid in planning release schedules to accommodate expected demand. To accomplish this a streamflow routing model must be used in conjunction with a soil moisture/evapotranspiration model.

Prior work in this area includes an agricultural irrigation Decision Support System (DSS) which can be used by a local water manager to estimate current field moisture conditions, streamflow, and water use priority (Allen, 1985). This model uses rather simple expressions to describe soil moisture and streamflow and was designed so that it could be run by a micro-computer thus making it accessible to water managers in small water districts. The DSS uses daily temperature, solar radiation and crop coefficients to determine the soil moisture. Streamflows are calculated using the linear reservoir technique given the inflows at the upper reaches and tributaries as well as diversions for irrigation. The DSS has been shown to accurately model field conditions given the required inputs. To be used as a predictive tool for water managers requires forecasts of the inputs, principally upstream inflow to the river system, precipitation, temperature and solar radiation. Given accurate forecasts a model such as the DSS has the potential for great utility in predicting irrigation water requirements. The streamflow portion of the model, when used in a forecasting mode, will indicate how much water will be available instream and can be used to determine how much of a shortage there will be or how much water must be released from a reservoir to meet demand. Such predictive capacity should enable the

water manager to make a more informed decision as to how much water to release, thereby increasing efficiency resulting in cost savings as well as increased available water.

OBJECTIVE

The objective of this research is to investigate and develop forecasting techniques for the inputs required by the DSS model. In addition, an improved streamflow routing model is developed to more realistically represent the river system and hydraulic processes. Of primary interest in this study are the effects of forecast errors on the overall predictive/operational characteristics of the system. Forecast and model errors are evaluated to determine the suitability of the forecast techniques. The effects of error propagation from the forecast into the soil moisture model and ultimately through the routing model are investigated to determine the behavior of the model error. Sensitivity analysis is used on the soil moisture model to determine which parameters and/or inputs have the greatest impact on the resulting water demand prediction. This knowledge will indicate which of the forecast inputs or parameters need to be most accurately estimated.

The soil moisture model requires daily temperature, solar radiation, and precipitation as inputs. Stochastic models are investigated and developed to forecast these variables. The models investigated include Markov chains, single and multivariate autoregressive models, and autoregressive-moving average models

(ARMA). Forecasts of streamflow are needed at upper reaches and tributaries in the system as inputs to the routing model. Stochastic methods of streamflow prediction are investigated and developed. To route streamflow, common routing techniques are investigated. A method of computation for a multiple reach system is presented using a discrete state-space formulation of the common Muskingum-Cunge river routing technique. This technique is somewhat more complex than the linear reservoir technique presently used in DSS but allows for much longer reach lengths resulting in fewer computations and maintaining correspondence of the method with other hydraulic techniques. Acceptable ranges of the routing parameters are also investigated. The state space formulation allows tracking the propagation of forecast error. This is developed for both the soil moisture and streamflow models. Using these results the forecast and model errors can be followed from the soil moisture model into the streamflow model. A first order sensitivity analysis is performed on the soil moisture model to determine the effects of forecast error specifically in this model.

CHAPTER II

FORECASTING MODELS

THE NEED FOR FORECASTS

Forecasting of weather and streamflow have many practical uses. Common uses of forecasts are for flood control, drought management and water supply for irrigation and industry. Much of the weather forecasting in the Pacific Northwest is used to determine flood magnitude so that control or evacuation measures may be taken to minimize loss. In other areas, climate forecasts are used to estimate drought severity so that water conservation plans may be developed. Accurate forecasts used for such purposes result in significant cost savings in operating efficiencies as well as loss minimization. Water supply forecasts can also be used to aid the normal day to day operation of a water resources project.

Through the use of the historic flow record, a water manager is able to develop sets of guidelines for reservoir operation. The guidelines, known as rule curves, specify minimum and maximum reservoir levels throughout the year based on the requirements of the project. For example, with a reservoir used for flood control and water supply, it is desirable to maintain the reservoir level low

enough so that flooding can be contained, yet not so low that water supply cannot be met. A flood study performed on the historic flow record or through simulation can be used to determine flood magnitudes that the project will be expected to accomodate throughout the year or flood season. This information is used to construct the flood control rule curve and thus an upper bound for the reservoir level. Knowledge of future water demand and system drought characteristics will allow a lower bound rule curve to be determined. Of course, it is possible for rules curves to suggest levels that are in conflict with each other such as a maximum level for water supply. This requires prioritization of project use. Once the rule curves are constructed, water supply forecasts can then be used to determine the appropriate releases such that the reservoir level is maintained between the levels specified, thus aiding the day to day operation of the project.

The climatic conditions in an area must be considered before any modeling can be done. Different types of hydrologic environments favor different models. In an area where snowpack supplies much of the streamflow it is possible to get a reasonable estimate of the amount of water that will be available during the latter part of the year by measuring snowpack and calculating the total volume of water present. With such information the water supply problem is reduced from the more general problem in which both quantity of water and temporal distribution must be determined to one in which only the temporal distribution is required. Through the use of models of snow fed systems, it is possible to start making seasonal volume runoff forecasts quite early in the season. The Streamflow Simulation and

Reservoir Routing Model (SSARR) developed by the North Pacific Division, U.S. Army Corps of Engineers (1972) for use in the Columbia River basin is such a model used primarily for flood control. This model uses estimated snowpack water content to determine total seasonal volume and then depletes this amount to streamflow as the season progresses based on temperature and precipitation forecasts. In the case of a precipitation fed system the situation is much more difficult. Neither the future amount of water nor the distribution in time is known with any certainty.

CLIMATE FORECASTING METHODS

Common forecasting methods for weather variables include meteorological and statistical methods. Meteorological forecasts incorporate weather patterns and the physical phenomena that govern the variables being measured. This method requires considerable meteorological data such as satellite photographs, pressure measurements, and humidity readings. Complex models are required to interpret this data and return a forecast. Even so, the results are often inaccurate due to factors that are missed or simply not included.

Statistical forecasting methods make use of the historic record to correlate future events to events in the past using an empirical model. More complex statistical models may also include the interrelationships between the variables. Stochastic models are generally fit to historic sequences and forecasting is based on a

conditional expected value. In addition, these models can be used to create synthetic data sets whose properties are like those of the historic record. These synthetic sets of data can then be used to simulate a hydrologic system and study its response under different sequences of climatic conditions.

The use of forecasts in this study is for application to irrigation water management. The weather forecasts are used with a soil moisture model to determine how much water is likely to be required by the crops in the future. The streamflow forecasting models are used in conjunction with the routing model to estimate streamflows. Given expected supply and demand of water at present and in the future a water manager can make appropriate releases so that demand is met without sending an excess of water resulting in waste or a shortage of water later on in the season. Ideally a manager would like to know all of the demands and all of the supply at the beginning of each year and be able to set the entire schedule from this knowledge. Unfortunately this is not yet possible as neither weather nor streamflow can be accurately predicted for each day over the entire growing season. However, shorter length forecasts can be made and these can certainly be used by a water manager to aid in the decision making process.

To demonstrate typical statistical properties of the proposed models, sets of data from the Tualatin Valley will be used. This basin is typical of western Oregon and isolated in the Willamette Valley of Oregon. The climate during the latter part of the growing season (May through September) is typically warm and dry. The

Tualatin River and its tributaries begin in low hills off the coast range and receive their water from rainfall with little significant flows resulting from snow pack. The model is only required during the growing season, thus the forecasting scheme is only for the period from 1 May through 30 September. The forecasting model for climatic variables consists of three major components. Precipitation models are considered separate from the temperature and solar radiation due to inherent differences in the nature of these variables.

STATISTICAL MODELS AND FORECASTING

The climate and hydrologic variables that are to be forecast for this system are periodic, or non-stationary, in nature. With a periodic time series, statistical properties such as the mean, variance, and skewness will vary throughout the year. Yearly streamflow is a good example of a stationary time series. Figure 1 shows a typical yearly (stationary) streamflow record with no discernable periodicities.

Figure 2 shows a typical monthly (periodic) streamflow record for the same river, and the monthly mean flows as determined from a 10 year data set, demonstrating the periodicities of within the year and in the statistics.

For the purpose of this research, daily forecast values are required. To simplify, and increase the number of points that will be used to estimate the sample statistics, thus decreasing the confidence interval, it is helpful to lump sets of daily values together. These

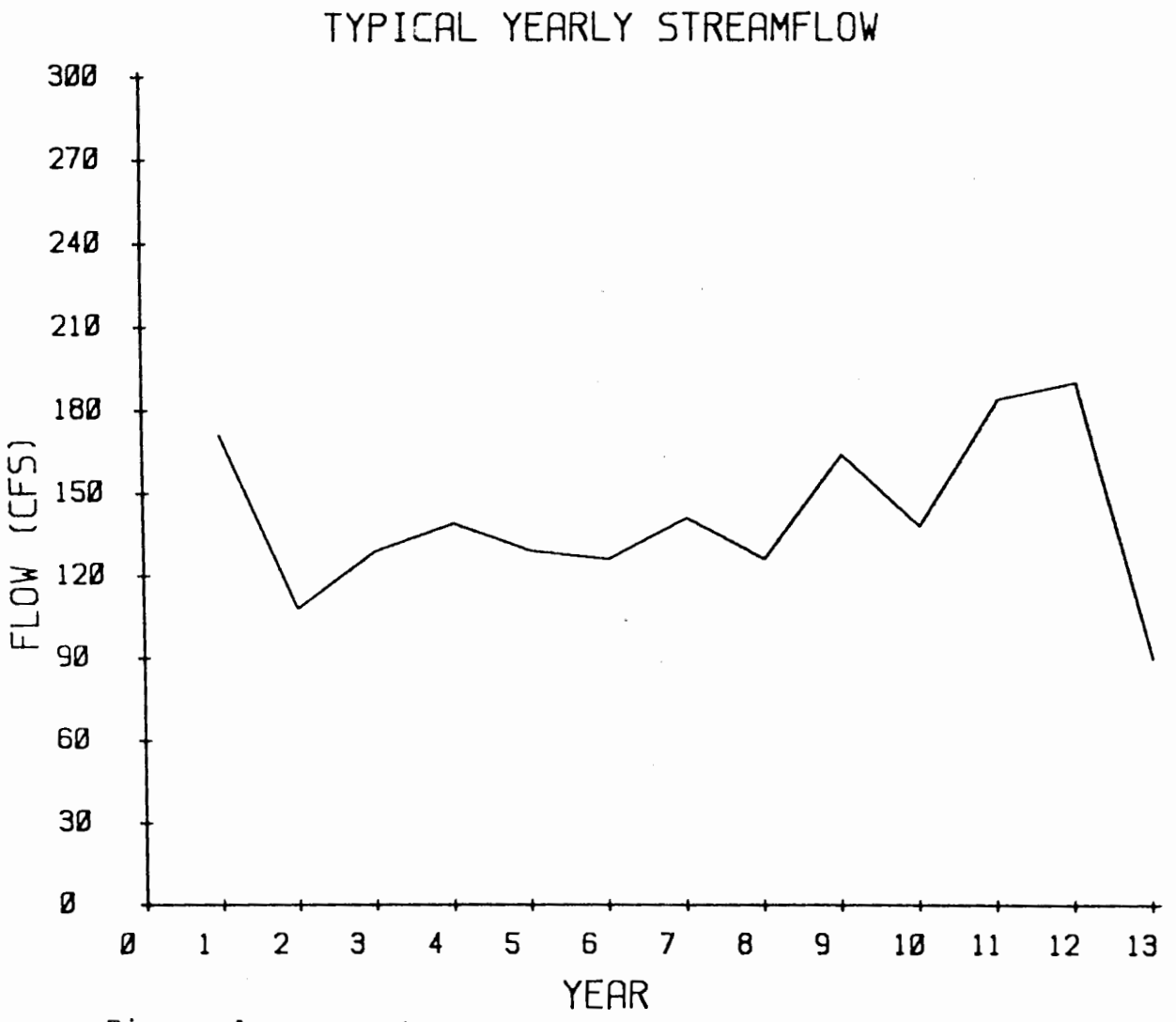

Figure 1. A typical yearly streamflow series exhibiting little or no periodicity.

sets are such that the statistical properties are not significantly different, or can be considered to be stationary, over the period. For example, one could calculate periodic mean daily values for a data set over a two week period as opposed to one for each day (Richardson, 1981). This is particularly useful for small data sets.

Many stochastic models are also based on the assumption that the variable to be modeled is normally distributed (Salas et al., 1980). For variables that are not normal, it is necessary to transform them in some manner. The transformation required may depend on the characteristics of the variable being modeled. Most stochastic models are used to model the residuals of the variables and are fit using a residual, or standardized, time series. A residual is defined as follows:

$$z(v,t) = (x(v,t) - \overline{x}(t))/\sigma(t) \qquad 2.1$$

where:

- $z(v,t)$ - residual of $x(v,t)$, the random variable
- $x(v,t)$ - data element
- $\overline{x}(t)$ - periodic mean of $x(v,t)$
- $\sigma(t)$ - periodic standard deviation of $x(v,t)$
- v - year index
- t - day index

The residual series of the data in figure 2 is shown in figure 3, demonstrating that much of the periodicity is removed by this process. Models presented in this chapter are for residuals of the variable and are transformed into actual values by multiplying by the standard deviation and adding the mean.

Stochastic models are frequently used to generate sets of data whose statistical properties are similar to those of the historic

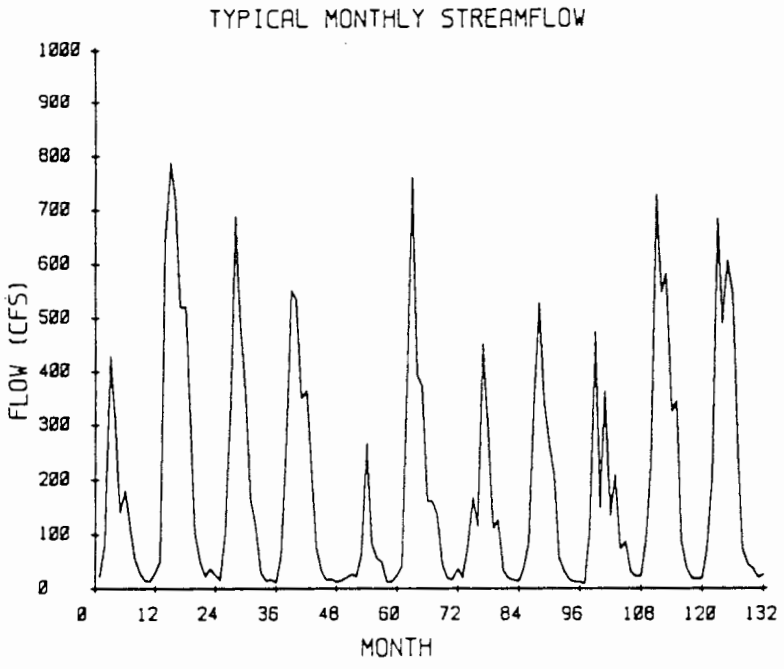

Figure 2. A typical monthly streamflow series showing within the year periodicities.

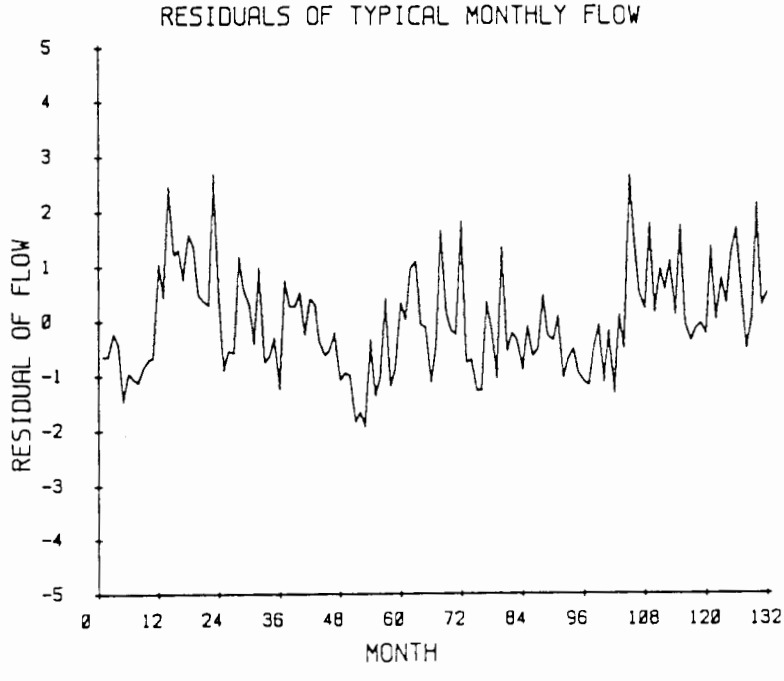

Figure 3. The residual streamflow series of the flows in Figure 2 showing removal of much of the periodicity.

data. These models typically involve terms modeled and a random noise term, $\varepsilon(t)$. Because of the random noise term, the generated sample paths cannot be expected to be the same as the actual occurrence. When forecasting using a stochastic model, the objective is to minimize the square of the deviations between the actual and forecast values (Box and Jenkins, 1976). In the case of a linear stochastic model this produces a minimum variance forecast. To simply forecast the mean for a variable would yield a variance that is the same as the sample variance. Using conditional expectation to forecast a variable $z(t)$, conditioned by the previous values of $z(t)$ we have:

$$z(L) = E[z(t+L) \mid z(t), z(t-1), \ldots] \qquad 2.2$$

where:

$z(L)$ - the forecast function at L time steps in the future

E - expected value operator

L - lead time of forecast

By taking the expectation of a generation model, the forecast function is obtained. This gives the minimum mean square error forecast for a given model, minimizing the variance of the forecast. ARMA models consist of terms relating future flow to past flow and past deviations in flow, as well as a random noise term. For models of this type where the random noise term is additive and has $E[(t)] = 0$, this results in an unbiased forecast as well (Box and Jenkins, 1976).

PRECIPITATION FORECASTING

Stochastic modeling of daily precipitation quantity is

considerably different from modeling temperature, solar radiation, and streamflow. Stochastic models such as autoregressive and autoregressive-moving average which can be used with monthly or yearly rainfall quantity and with temperature, solar radiation and streamflow do not work well with daily precipitation (Richardson, 1981). These models require that the random variable be continuous and normally distributed or that it can be transformed so that it is normal. However, daily precipitation quantity is intermittent, containing many zero values and cannot be easily transformed so that an approximate normality results. Furthermore, there is typically very little persistence even in a wet sequence, often one day is as much as can be observed. The persistence is even less for precipitation quantity assuming that one could forecast the wet or dry status of a day. For these reasons a precipitation model is presented that is quite different from the types of temperature, solar radiation, and streamflow models.

Markov Chains and Processes

First order Markov chains are often used to describe both precipitation occurrence and precipitation quantity (e.g. Todorovic and Woolhiser, 1974, Khanal and Hamrick, 1974, and Bruhn, Fry, and Fick, 1980). A Markov process is one in which the probability that the system will be at a given state X at time t, may be determined from the prior states of the system. For an nth order Markov chain this is written as:

$$P[X(t) = x(t) \mid X(t-1),\ldots,X(1) = x(1)]$$
$$= P[X(t) = x(t) \mid X(t-1) = x(t-1),\ldots,X(t-n) = x(t-n)] \qquad 2.3$$

for all: $X(i)$; $i = 1, 2, 3\ldots$

$t < n$

where:

p - probability operator

A first-order Markov chain is written as:

$$P[X(t) = x(t) \mid X(t-1) = x(t-1),\ldots,X(1) = x(1)] \qquad 2.4$$
$$= P[X(t) = x(t) \mid X(t-1)]$$

which provides the simple day to day transition probabilities (Khanal and Hamrick, 1974). In this case the state, x(t), is either the depth of rainfall on a given day or simply the occurrence of rainfall.

Thus, the probability of the system being at any given state (rainfall depth) depends only on the state of the system at the preceeding time period. Lack of persistence in precipitation usually dictates that the order of the chain be one but sometimes greater persistence is found. This formulation is for discrete states. Therefore, for the purpose of precipitation modeling it is necessary to discretize the range of probable daily precipitation depths. To accomplish this, the range of values as well as the occurrences of the less frequent values and the degree of discretization that is required must be considered.

Development and application of Markov chains to precipitation modeling can be accomplished by several approaches. In some instances the precipitation states are chosen and the transition probabilities are calculated from historical data for each of the states providing a

discrete transition probability distribution for each state. When used for data synthesis, modeling is performed using these distributions by choosing the state for day t+1 at random as dictated by the calculated transition probabilities given the state on day t (Khanal and Hamrick, 1974). Alternatively an approach is used in which only the wet or dry status of day t+1 is modeled using the Markov chain and the quantity of precipitation is modeled using a gamma distribution or some other continuous distribution with properties similar to those found in the precipitation record (Bruhn, Fry, and Fick, 1980). In this case the wet or dry status of day t+1 is chosen at random as dictated by the transition probabilities. If day t+1 is found to be wet then the magnitude of the precipitation is chosen at random from an appropriate distribution.

These Markov chain methods are quite useful for synthesizing data and have been shown to produce records that exhibit behavior quite similar to the historical record (Khanal and Hamrick, 1974). For the purpose of forecasting it is not reasonable to randomly select the state of the day from the distributions whether derived from Markov probabilities or from some other distribution. To forecast, the expected value of the state given the previous state should be used. To determine what should actually be forecast, it is useful to investigate the precipitation characteristics of the data.

To determine the first order transition probabilities, letting i be the state on day t, and j be the state on day t+1, the transition frequencies, $f_{i,j}$ are determined by simply counting the times during the historic record that a transition from each state on one day is

followed by another state on the following day for each of the periods that can be considered to be stationary. Table I shows a tabular arrangement of transition frequencies. Each cell contains the number of times that a transition was made from the state of the row of the cell to the state of the column of the cell. By summing across each row, the frequency of occurrence for each state, F, is found.

$$F_i = \sum_{j+1}^{n} f_{i,j} \text{ for all states on day t, i=1 to n} \qquad 2.5$$

A set of these frequencies will be needed for each of the periods. The transition probabilities are then found by dividing each of the transition frequencies by the total number of occurrences of the corresponding row, F_i.

$$P_{i,j} = f_{i,j} / F_i \qquad 2.6$$

The state to forecast for day t+1 is found by multiplying the probability of each cell by the value of the state for that cell. The forecast, or expected value of precipitation quantity, x(t+1) is:

$$x(t+1) = \sum_{j=1}^{n} P_{ij} x_j \qquad 2.7$$

Where x_j is the mean of the rainfall depth range for state j. Table II shows the transition probabilities, as would be determined from the transition frequencies, as well as the value to forecast for day t+1 given the state at t. Each cell here is the probability of a transition of the state in the row of the cell to the state of the column of the cell.

TABLE I
TRANSITION FREQUENCIES

State on day t	State on day t+1 1	2	3	•	n	
1	f_{11}	f_{12}	f_{13}	•	f_{1n}	F_1
2	f_{21}	f_{22}	f_{23}	•	f_{2n}	F_2
3	f_{31}	f_{32}	f_{33}	•	f_{3n}	F_3
•	•					
•	•					
•	•					
n	f_{n1}	f_{n2}	f_{n3}		f_{nn}	F_n

TABLE II
TRANSITION PROBABILITIES
AND FORECAST VALUES

State on day t	State on day t+1 1	2	3	•	n	Forecast
1	p_{11}	p_{12}	p_{13}	•	p_{1n}	$\sum_{j=1}^{n} p_{ij}x(j)$
2	p_{21}	p_{22}	p_{23}	•	p_{2n}	$\sum_{j=1}^{n} p_{2j}x_j$
3	p_{31}	p_{32}	p_{33}	•	p_{3n}	$\sum_{j=1}^{n} p_{3j}x_j$
•	•					
•	•					
•	•					
n	p_{n1}	p_{n2}	p_{n3}		p_{nn}	$\sum_{j=1}^{n} p_{nj}x_j$

TEMPERATURE AND SOLAR RADIATION FORECASTING

Several stochastic models can be applied to describe temperature and solar radiation. As with precipitation the amount of persistence in these variables greatly affects the ability to forecast them. Models for both temperature and solar radiation are presented together because they can be adequately represented with the same models, unlike precipitation. Both processes are continuous random variables. For this study forecasts for up to seven days are used. Since the model must operate within the year and these variables exhibit a seasonal variation, the periodicity of the data must be considered. This tends to complicate the models somewhat and in the case of high order models tends to make parameter estimation rather cumbersome.

There is an obvious physical relationship between temperature and solar radiation. One would typically expect that high temperature would be associated with high levels of solar radiation and vice versa. Analysis of historic records of temperature and solar radiation show this to be true as they exhibit relatively high values of covariance as is demonstrated in chapter five. For this reason it is desirable to use forecast models that will preserve this covariance and provide for more realistic forecasts. Multivariate models are capable of doing this and are investigated.

Multivariate Autoregressive Models

Multivariate autoregressive models (MVAR) can be used to model

temperature and solar radiation together (Richardson, 1981). The model uses not only the autocorrelation coefficients as in the univariate autoregressive (AR) model but includes the cross-correlation between variables. The MVAR model degenerates to an independent set of AR models in the case where there is no cross-correlation between variables. It is intuitively apparent that there is a relationship between temperature and solar radiation so the use of a model that incorporates this relationship should be able to provide more realistic results than a model that considers the two separately.

The periodic model is of the form:

$$\underline{z}(v,t) = [\underline{A}(t)\ \underline{z}(v,t-1) + \underline{B}(t)\ \underline{\varepsilon}(v,t)] \qquad 2.8$$

where: $\underline{z}(v,t)$ - vector of residuals of variables to be modeled

$\underline{A}(t)$ - coefficient matrix

$\underline{B}(t)$ - coefficient matrix

$\underline{\varepsilon}(v,t)$ - random noise vector having the property $E[\varepsilon(v,t)] = 0$

The $\underline{A}(t)$ matrix is defined as:

$$\underline{A}(t) = \underline{M}_{1,t}\ \underline{M}^{-1}_{0,t-1} \qquad t=1 \text{ to number of periods} \qquad 2.9$$

with B(t) defined such that:

$$\underline{B}(t)\underline{B}(t)^T = \underline{M}_{0,t} - \underline{M}_{1,t}\ \underline{M}^T_{0,t-1} \qquad t=1 \text{ to number of periods} \qquad 2.10$$

with $\underline{M}$ being the correlation matrix given by:

$$\underline{M}_{k,t} = \begin{bmatrix} r^{11}_{k,t} & r^{12}_{k,t} & \cdots, & r^{1n}_{k,t} \\ r^{21}_{k,t} & r^{22}_{k,t} & \cdots, & r^{2n}_{k,t} \\ \cdot & \cdot & & \cdot \\ \cdot & \cdot & & \cdot \\ \cdot & \cdot & & \cdot \\ r^{n1}_{k,t} & r^{n2}_{k,t} & \cdots, & r^{nn}_{k,t} \end{bmatrix} \qquad 2.11$$

where: $r^{ij}_{k,t}$ - correlation coefficients between variables i and j for period t and lag k.

(Salas et al., 1980)

These relationships are used to estimate $\underline{A}(t)$ and $\underline{B}(t)$ based on moment estimates of $\underline{M}_{0,t}$ and $\underline{M}_{1,t}$.

To obtain the minimum variance forecast from this model, the conditional expectation is taken resulting in:

$$E[\underline{z}(v,t) \mid \underline{z}(v,t-1)] = [\underline{A}(t)\ \underline{z}(v,t-1)] \qquad 2.12$$

where:

$$\underline{z}(v,t) - \begin{bmatrix} RT(v,t) \\ RS(v,t) \end{bmatrix}$$

RT(v,t) - residual of temperature

RS(v,t) - residual of solar radiation

The response of this forecast approaches the mean values of the variables as the length of the forecast increases.

To improve upon this model one can incorporate the wet or dry status of the days being modeled as determined by the precipitation forecasting model (Richardson, 1981). This change in the model makes good intuitive sense as it allows there to be a different set of

parameters for wet days than for dry days. For both temperature and solar radiation this incorporation is beneficial. Typically one will find solar radiation to be decreased due to the cloud cover on a day precipitation occurs and temperature is generally lower when there is a precipitation occurrence.

With this model the means and standard deviations are found from the historical record for both the wet days and the dry days. The residual series is computed conditioned by the wet or dry status of the day and the correlation structure is determined from this series. This is of the form:

$$\underline{x}(i,v,t) = [\underline{A}(t)\ \underline{z}(i,v,t-1)]\ \underline{\sigma}(i,t) + \underline{\mu}(i,t) \qquad 2.13$$

where:

$\underline{\sigma}(i,t)$ - standard deviation matrix for condition i
$\underline{\mu}(i,t)$ - mean matrix for condition i
i - condition indicator: 0 = dry, 1 = wet

Note that this model is written in terms of actual values and not residuals. This is due to the inclusion of the wet or dry conditioned mean and standard deviation.

Autoregressive-Moving Average Models

Autoregressive-moving average models of order p and q, ARMA(p,q), can be used to model temperature and solar radiation. These models, and the subset referred to as autoregressive models, AR(p), are often used in single-variate form which for the case of temperature and solar radiation would not be able to include the correlation between them. Multi-variate formulations are available for AR models which are relatively simple for low order models but get extremely complicated and cumbersome for higher order models.

Approximate multi-variate forms of ARMA models are available but are complicated and cumbersome for higher order models with relatively little utility beyond that of an autoregressive model. Based on the experience of other investigators (e.g. Richardson, 1981) and the ease of implementation, the first order multi-variate autoregressive model is selected as the model for temperature and solar radiation in this study.

STREAMFLOW FORECASTING

Many methods are available for use in forecasting streamflow. The degree of sophistication required in the model is determined by the properties of the river basin, the forecasting needs of the project as well as by the resources available to operate the model. Physically based models in which all of the physical processes governing the motion of the water through a watershed are described by partial differential equations are far too computationally difficult to apply to an entire watershed. In addition, Loaque and Freeze (1985) have shown that this approach has questionable value for prediction. Alternately, large, complex models such as the SSARR model (Army Corps of Engineers, 1975) are designed to forecast the streamflow of an entire watershed. In this model physical processes such as surface flow, subsurface flow, and base flow are accounted for conceptually. These three components of flow are then routed to the stream using the linear reservoir routing technique. The methods by which they are accounted for are not specifically derived from the actual physical

characteristics of the watershed, i.e. soil type, but are empirically derived for simplicity. Thus, this type of model is empirical yet attempts to preserve at least some of the physical phenomena that occur within a watershed. Such simplification greatly reduces the amount of data that are required regarding the watershed when compared to a truly physically based model. Another popular watershed model is the Stanford Model developed by Crawford and Linsley which has had many improvements since it was introduced. This model was designed to be used in all types of watersheds and is also of the empirical nature.

Both of these models as well as most general watershed models require moderately large computer resources, large amounts of data, and trained personnel for application. These models are far too costly and complex for use in local water management. Stochastic models can be much less complicated yet may be capable of providing the desired forecast accuracy. Several alternative major stochastic models are investigated below and evaluated for their suitability with the system being modeled.

Review Of Stochastic Streamflow Models

There are several stochastic models that have been used to model streamflow. Many of these models are well suited for synthesizing sets of yearly or monthly data but tend to be less realistic when applied to daily or shorter time period models. The reason for this is the asymmetric nature of daily flow patterns. A precipitation event often will cause a rather rapid jump in the streamflow

hydrograph. Flows then receed at a much slower rate due to the nature of the hydraulics of the system. In order to produce realistic daily flow records or forecasts this behavior must be considered. Figure 4 is a typical May through September daily streamflow record for the Tualatin River and clearly demonstrates the asymmetric nature of daily flow. Models that have been used for the synthesis of daily streamflow are the AR, ARMA, shot-noise, Markov, and transfer function. They each have some advantages and disadvantages which are examined.

Autoregressive-Moving Average Models

Mixed autoregressive-moving average models (ARMA) and the subset autoregressive models (AR) are probably the most commonly used form of stochastic streamflow models. Periodic AR models of order p have the form:

$$z(v,t) = \sum_{i=1}^{p} \phi_i(t)\, z(v,t-j) + \varepsilon(v,t) \qquad 2.14$$

and the form of an ARMA model with orders p and q is:

$$z(v,t) = \sum_{i=1}^{p} \phi_i(t)\, z(v,t-i) - \sum_{j=1}^{q} \theta_j(t)\, \varepsilon(v,t-j) + \varepsilon(v,t) \qquad 2.15$$

where: $z(v,t)$ - periodic residual of modeled value
$\phi_i(t)$ - ith periodic autoregressive parameter
$\theta_j(t)$ - jth periodic moving average parameter
$\varepsilon(v,t)$ - independent and indentically distributed random variables with $E[\varepsilon(v,t)] = 0$

The popularity of these models is partially due to the physical justification (Salas et al. 1980). AR models are quite good during the flow recession portion of a year where streamflow results

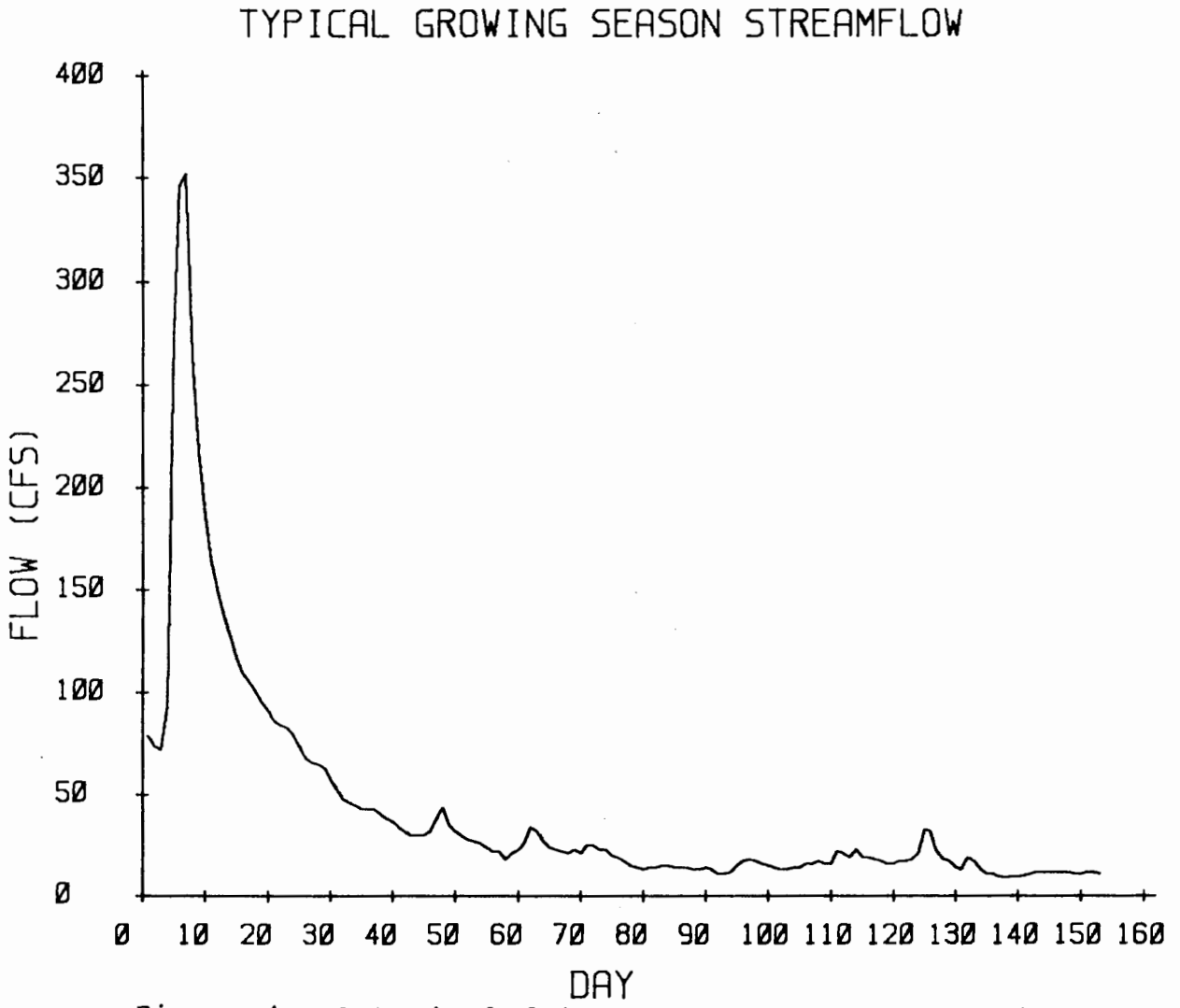

Figure 4. A typical daily summer streamflow series exhibiting the asymmetric nature of daily streamflow.

primarily from groundwater. These models base future streamflow as a fraction of the current streamflow. During periods of high flow the flows are primarily the result of rainfall, snowmelt, or both which can be modeled as a disturbance to the system by the moving average component of the model. This adds a portion of the randomness of the previous flow to future flow. When combined the model is good for use during both of the flow patterns.

Obtaining the minimum variance forecast from these models is quite simple and involves taking the expected value of the generation model. This simply eliminates the random noise, $\varepsilon(v,t)$ term from equation 2.14 since $E[\varepsilon(v,t)] = 0$.

Parameter estimation for these models can become computationally difficult especially in the case of high order seasonal models. Box and Jenkins (1970) describe parameter estimation techniques for these models as do Salas, et al. (1982) for seasonal models. It is often possible to model a lower order ARMA with a higher order AR model which may often be easier to fit than the ARMA model. To determine the type and order of model the Akaike Information Criterion (AIC) can be used. The AIC calculated for ARMA models is written as:

$$AIC\ (p,q) = N \ln (\sigma_\varepsilon^2) + 2(p+q) \qquad 2.16$$

where: N - sample size

σ_ε^2 - maximum liklihood estimate of the residual variance

The model with the lowest AIC value is chosen as the best one. This method is basically weighing the increased complexity of the model in terms of the number of parameters against the improvement in the residual variance.

The major drawback to using this class of models to synthesize or forecast daily flows is that they produce records that do not look like typical daily flow hydrographs. ARMA models produce symmetric sequences which are reasonable yearly and monthly models but may not be realistic for daily models.

Markov Chains and Processes

Multi-state, multi-lag Markov models have been found to provide reasonable sequences of daily streamflow data (Yakowitz, 1979). These models are much the same as described for precipitation above but will always use several states or possibly a continuous model and commonly use more than one lag for determining the streamflows, both of which add considerably to the complexity of model development. Forecasts of streamflow are made by taking the expected value of streamflow as dictated by the transition probabilities. The major advantage is that realizations of the process look like actual streamflow records and there is no need to select a specific distribution to model the flows. The distributions are reflected in the transition matrices as determined from the historical record. The major drawbacks include computational difficulty in fitting the model and the determination of model and forecast errors which are required in this study.

Shot Noise Processes

Shot noise models are often used to generate sequences of streamflow and are capable of producing sequences that visually resemble actual daily streamflow records (O'Connell, 1979). Several types of these

models are used. The typical shot noise model generates events of random magnitude at random times. Events are defined as disturbances to the system which, in the case of streamflow, would result from precipitation, snowmelt or both. Timing of events is typically determined by a Poisson distribution and the magnitude is usually determined by an exponential distribution. Once the timing and magnitude of the event is determined then it is allowed to decay at a rate that is consistent with recession rates found in the river system. The decay is usually modeled with an exponential function. The form of a single shot noise model is:

$$X(t) = \sum_{m=N(-\infty)}^{N(t)} y_m \, e^{-b(t-\tau_m)} \qquad 2.17$$

where: y - jump height as determined by an exponential function
τ_m - random time of event occurrence
$N(t)$ - number of events occurring in (0,t), generated by a Poisson process
b - a parameter
$x(t)$ - initial value of the process at time t=0

This is the sum of all the pulses up to time t, decayed by the exponential function.

The major advantage of shot noise models over more commonly used models, such as the ARMA model, is the asymmetric sample paths which more closely resemble actual daily streamflows. One drawback of this model is the inability of it to produce realistic recessions. To make the model more realistic two components can be modeled, one representing the rapid decay as would be found shortly after a precipitation event due to surface flow and one decaying more slowly representing baseflow recession (O'Connell, 1979). Other improvements

to this model include the second orcer shot noise model which involves one event rate for both of the events of the double shot noise model. This model is somewhat simpler than the double shot noise model and has been found to represent flows quite realistically. Another type of shot noise model breaks the recession into two parts (Sargent, 1979). The first decay function is rapid consisting of a power function. The second, slower part of the recession is modeled with an exponential function. This form produces flows that look more reasonable than the single shot noise model and is quite comparable to the double shot noise model. The parameters of this process are somewhat more difficult to estimate and the break between the two recession functions is difficult to determine.

When used to forecast streamflows this model would be of little utility. The timing of the events would no longer be randomly spaced since they are to represent some sort of input event. These events would need to be correlated to streamflow magnitude in some manner which there seems to be little basis for doing with this type of model. Furthermore, this correlation would most likely be much like trying to fit some sort of transfer function model yet would be less realistic due to the nature of the recession modeling.

Transfer Function Models

The transfer function incorporates some form of input which is usually linearly related to streamflow. In one such model (Miller, Bell, Ferreiro, and Wang, 1981) streamflow was modeled as a function of past flows, present and past precipitation, and the square of the

present precipitation. In the application presented, this model performs better, in a forecasting model, than the time series models. This specific model has the following form:

$$\ln Q(t) = \beta_0 + \beta_1 \ln Q(t-1) + \beta_2 \ln Q(t-2) + \beta_3 R(t) + \beta_4 R(t) + \beta_5 R(t-1) + \beta_6 R(t-2) + N(t)$$

where: $Q(t)$ - flow at time t
$R(t)$ - standardization of rainfall at time t
$N(t)$ - random noise
β_i - ith regression coefficient; i = 1 to 6

It seems reasonable that this type of model should out perform time series models due to the inclusion of precipitation as a forcing function. However, for use in forecasting the precipitation quantities in the future would be required, which is not a trivial problem as noted above. Choice of what should be included as a forcing function as well as the appropriate transformation are not necessarily simple as can be seen by the seemingly arbitrary form of the model above. This model was fit to the data using least squares. Box and Jenkins (1970) provide further parameter estimation techniques for use with transfer functions.

Streamflow Model Selection

The final choice of a model to be used for forecasting should be made based on the forecasting needs, the resources available to fit the model, and the characteristics of the system being modeled. For the test data set that is being used in this study, Tualatin River, near Gaston, Oregon, an inspection of the flow patterns from May through September was performed. During this period it is apparent

that the general flow pattern indicates flow recession. There seems to be nosignificant jumps in streamflow following the precipitation that occurs during this period. From this it is apparent that a transfer function type of a model would not be appropriate as there is no input to drive the system. For the same reason a shot noise model would also not be appropriate. A Markov model could be used but as mentioned before, error analysis which is essential to this study would be difficult to perform. Since the flow is in recession, it should be able to be modeled for forecasting satisfactorily using an AR or ARMA type of a model. For these reasons the AR and ARMA models are chosen for further investigation as the forecast models for this system. Several models of different orders are fit and the best is determined using the AIC.

CHAPTER III

SYSTEM MODELS

The components of a water management model investigated in this study consist of a physically based routing procedure driven by forecast tributary inflow and irrigation demands, and a soil moisture model driven by the forecasts of temperature and solar radiation. These components, when combined with an irrigation management system such as the DSS (Allen, 1985), and the forecasting models of Chapter II can provide information that aid in planning of irrigation timing and quantity several days in advance. To determine the adequacy of these forecast models it is necessary to investigate their errors and how these errors propagate through the system. This chapter develops a state space approach to the Muskingum streamflow routing technique and presents the simplified soil moisture model (Koch and Allen, 1985) in notation which facilitates analysis of errors and error propagation.

STREAMFLOW ROUTING

For most water supply systems, the demands for water are to be met by either existing streamflow, releases from the reservoir, or both. In order to ensure adequate water availablity in the stream at any given time some method of accounting for streamflow must be

provided. The routing model must be developed so it is complete enough to accurately describe the flow in the system yet simple enough to be computationally efficient. In this section we will review the physical processes involved in streamflow and present a model meeting these criteria.

For this system the streamflow routing will be driven by two inputs, upstream flows in the main stream and tributaries, and irrigation diversion demands as dictated by the soil moisture model. The effects of errors in these inputs are evaluated for the model.

Fundamental Flow Equations

For a one-dimensional, straight channel, with no lateral inflow, the flow can be described by the Saint-Venant equations of continuity and momentum, respectively:

$$\partial h/\partial t + \partial(uh)/\partial t = 0 \qquad 3.1$$

$$\partial u/\partial t + u\partial u/\partial x + g\partial h/\partial x = g(S_0 - S_f) \qquad 3.2$$

Where:

- h - local depth of flow
- t - time
- u - velocity of flow
- x - axis in direction of flow
- g - acceleration due to gravity
- S_0 - bottom slope
- S_f - friction slope

The terms of these equations have the following physical significance:

- $\partial h/\partial t$ - change in depth with respect to time
- $\partial(uh)/\partial t$ - change in flow with respect to time
- $\partial u/\partial t$ - local acceleration due to unsteadiness in the flow

$u\partial u/\partial x$ - convective acceleration due to nonuniform nature of the flow

$g\partial h/\partial x$ - acceleration caused by the pressure gradient

These are nonlinear partial differential equations which have no general analytical solution. For this reason it is necessary to either simplify these equations to a form with a known analytical solution which still provides a reasonable representation of the flow, use some numerical approach on the original equations, or use both a simplification and a numerical approach together. Two common simplifications of the full dynamic wave equation are the diffusive and the kinematic wave.

Diffusive Wave. Here the local and convective acceleration terms are considered to be negligible compared to the frictional, gravitational, and pressure terms. The momentum equation then takes the form:

$$S_f = S_o - \partial h/\partial x \qquad 3.3$$

By manipulating equation 3.1 and 3.3 one obtains:

$$\partial h/\partial t + c\ \partial h/\partial x = \mu d^2h/d^2x \qquad 3.4$$

where:

c - wave celerity = 1.5 u

μ - diffusive coefficient = ud/2S

This model produces some diffusion but not as much as the full dynamic wave. The diffusive assumption is reasonable in situations having mild slopes and long flood wave periods (Ponce, Li, and Simons, 1978).

Kinematic wave. In this model the inertial terms are neglected as is the pressure term. This model produces no diffusion and the form of the momentum equation is:

$$S_o = S_f \qquad 3.5$$

which implies a uniform flow. A relationship between friction slope and discharge can be expressed through either the equation of Chezy:

$$Q = CA(RS)^{1/2} \qquad 3.6$$

or Manning:

$$Q = 1.486/n\ AR^{2/3}\ S^{1/2} \qquad 3.7$$

where:

Q - volume flow rate
C - Chezy coefficient
n - Manning's coefficient
R - hydraulic radius
A - area of flow

In general, this leads to an area discharge relationship of the form:

$$Q = a\ A^{b} \qquad 3.8$$

By manipulating equations 3.1 and 3.6 one obtains:

$$dQ/dA = budQ/dx \qquad 3.9$$

The kinematic approximation is valid for very mild slopes and waves of very long periods as would be typical of overland flow or flow in some river systems (Ponce et al. 1978). This approximation is more restrictive than the diffusive wave.

Analytical solution of the kinematic equation yields a solution with convection and no diffusion. However, using a finite difference scheme to solve the equation results in numerical inaccuracies which cause the result to exhibit both convection and diffusion. Cunge (1969) equated these numerical inaccuracies to the physical diffusion that should actually occur in a diffusive wave. In doing this he developed the well known, but empirically based, Muskingum routing technique thus giving a physical basis to the parameters used in the Muskingum technique.

Muskingum Routing

In the 1930's the Muskingum routing technique was empirically developed based on the storage equation and the assumption that the storage in a reach at any given time was a function of the inflow and the outflow.

$$dS/dt = I-O \tag{3.10}$$

and $$S = K[xI + (1-x)O] \tag{3.11}$$

where:

S - storage in a reach
I - instantaneous inflow
O - instantaneous outflow
K - a parameter
X - a parameter

This equation implies that there is a one to one relationship between storage or depth in the river and discharge as would be the case for the kinematic wave. The analytical solution would yield no diffusion of the flood wave. With the Muskingum method this is not the case as some diffusion does occur, apparently due to the fact that instead of the continuous form of the continuity equation a discrete form was used.

$$(I_1 + I_2)/2 - (O_1 + O_2)/2 = (S_2 - S_1)/\Delta t \tag{3.12}$$

For a multiple reach system, the solution is:

$$Q_{j+1}^{n+1} = C_1 Q_j^n + C_2 Q_j^{n+1} + C_3 Q_{j+1}^n \tag{3.13}$$

with:

Q_j^n - flow

J - space increment counter (reach)
n - time increment counter
$C_1 = (-KX + 0.5\Delta t)/(K - KX + 0.5\Delta t)$
$C_2 = (KX + 0.5\Delta t)/(K - KX + 0.5\Delta t)$
$C_3 = (K - KX + 0.5\Delta t)/(K - KX + 0.5\Delta t)$

The parameters K and X are commonly determined by choosing a value for X, usually close to 0.2 and then plotting storage in the reach verses [XI + (1 - X)O] for a given set of inflow and outflow data. The plots will be in the shape of a loop. This is done for several values of X. The plot with the narrowest loop has the most accurate value of X, and K is the reciprocal of the slope of a line drawn through the loop (Viessman et al. 1977). This method is somewhat cumbersome and the results are only good for floods with similar properties to the flood used for calibration. By equating the actual diffusion to the numerical diffusion Cunge (1969) found the values of K and X to be related to the properties of the physical and hydraulic system:

$$K = \Delta x/c \qquad 3.14$$

$$X = 1/2\ (1 - (Q/BS_0c\Delta x)) \qquad 3.15$$

where:

Q - flow rate
c - flood wave celerity = dQ/dA
A - cross sectional area of river
Δx - length of routing reach
B - width of the river
S - channel slope

Such basis makes parameter estimation much simpler and also allows for parameters to vary with different floods as needed if this is found to be a significant problem. Thus the parameters K and X depend on physical characteristics of the river and the flood of interest (since c, Q, B and S change both with respect to time and distance) as well as the time and space intervals. For the model to be physically realistic and produce diffusion it is necessary that the value of X be between 0 and 0.5.

Linear Reservoirs. A common simplification of the Muskingum routing technique is to set X = 0. The resulting equation sets the storage as a linear function of flow and is known as the linear reservoir. This model implies a "level pool" assumption which means that the water level in the reaches is assumed to be approximately level and flows as a system of cascaded reservoirs. This further implies that the reach lengths must be relatively short so that they may be considered level. For the physical basis of the model to be maintained, the reach length becomes fixed from Eq. 3.15 at:

$$\Delta x = Q/(BcS_0) \qquad 3.16$$

Time and Space Steps. From use and empirical testing it has been found that the choice of the space and time increments have a substantial impact on the results of the routing and must be chosen in such a manner as to yield realistic results (Ponce and Theurer, 1982).

From a practical standpoint it is apparent that the time increment, Δt, must be small enough so that the flood of interest is not 'lost' between two time steps. As a generally accepted rule of thumb it is recommended that there be at least 5 timesteps on the rising portion of the inflow hydrograph (Ponce and Theurer, 1982). No theoretical lower limit has been found for the time step and is usually set by the computational resources used to perform the routing computations as well as the appropriate time step required by the project.

The value of the space interval, Δx, also called the reach length, is more difficult to determine. Ideally one would like to have Δx be the distance from the inflow to the point of interest for

only one space step. However, empirical studies have shown that large values of Δx tend to produce flows downstream that are below baseflow. This is clearly unrealistic and the reach length must be chosen so that this 'dip' is either not present or is insignificant. The object becomes choosing Δx as large as possible without causing unrealistic flows. From experimentation, Ponce and Theuer (1982) have found that the coefficient C_2 is solely responsible for the "dip" and will cause it to occur when C_2 is negative.

In terms of the Courant number, C:

$$C = c\Delta t/\Delta x$$

and the cell Reynolds number, D:

$$D = q/(S_0 c\Delta t)$$

the condition $C + D = 1$ should yield acceptable results. Greater restrictions can be placed on C_2 to provide a 'factor of safety' against the dip. In general this leads to:

$$C + D = \geq \varepsilon \qquad 3.17$$

$$\varepsilon > 1$$

This condition requires that:

$$\Delta x < 1/\varepsilon \ (c\Delta t + Q/BS_0 c) \qquad 3.18$$

Koussis (1982) has shown that theoretically $\varepsilon = 1$ but Ponce and Theuer suggest that a value of $\varepsilon = 2$ should be used thus providing a factor of safety. For the linear special case where $X = 0$, known as the linear reservoir routing method, the choice of Δx becomes fixed at:

$$\Delta x = Q/BS_0 c \qquad 3.19$$

which also serves as a lower bound for the general case since the

parameter X must not be less than zero. Depending on the characteristics of the river, the reach lengths may need to vary in order to satisfy the inequalities.

Due to the fact that Δt and Δx are related and that each has bounds which limit its range, it is possible that a choice for one variable within its range will lead to the other one being outside of the respective range. For this reason it may be necessary to iterate between them until both values are within their respective ranges. In summary:

$$0 < \Delta t < T/5 \quad \text{where} \quad T = \text{time of rise of hydrograph, and}$$
$$Q/BS_0c < \Delta x < 1/2$$

If one of these inequalities cannot be met then a smaller value for Δt is chosen and Δx is recomputed. These provide reasonably conservative limits.

Linear Reservoirs Vs. Muskingum. Using a linear reservoir approximation, the time increment is set in the same manner as in the Muskingum routing. The space increment, however, is set specifically at the lower limit of the Muskingum reach lengths as shown by Eq. 3.19. Requiring specific interval lengths with linear reservoir routing can cause considerable inconvenience if the reach lengths do not occur at the points of interest along the river. Also the resulting reach lengths are often relatively short. Note that with Muskingum reaches, during high flows and shallow slopes the upper limit for Δx can become quite large thus allowing for far fewer reaches than in linear reservoir routing if desired. Since Muskingum reach lengths are allowed to be within a range of values it is easier

to find reach lengths which correspond to points of interest along the river system without losing accuracy. The maximum allowable reach lengths can also be considerbly longer than the minimum of linear reservoir reach lengths depending on the physical characteristics of the river thus allowing for far fewer reaches and substantially less computation time. The Muskingum method also provides a greater degree of accuracy than the linear reservoir approximation because changes in celerity that occur undoubtedly lead to an incorrect linear reservoir reach length whereas this is not necessarily true with Muskingum routing. From Eq. 3.16 it can be seen that the value of Δx for a linear reservoir is based on both the celerity and the flow. One could theoretically change the reach length as required by the changes in the flow but this would require considerable data about the entire river system and would complicate calculations immensely. From this it is evident that the exact reach length is not maintained except at the discharge chosen for setting the reach length which means the physical correspondence is also not maintained. This flow, known as the reference discharge, is chosen as a representative flow in the reach. The selection is somewhat subjective and the problem can be averted by using Muskingum routing and a conservative value for a reference discharge. This gives a factor of safety against obtaining a reach length that is physically unrealistic. For all of these reasons the Muskingum routing procedure is preferred to the linear reservoir approach. This method is further developed using a state space formulation and solution to equation 3.13.

CONSTANT VS. VARIABLE PARAMETERS

Thus far, all of the discussion has been limited to the case where the parameters K and X are considered to be constant. This is not the case as both K and X are defined in terms of the wave celerity which is a function of flow and the flow rate itself. Unless flow is found to increase linearly with area then the celerity will not be a constant. When using Muskingum routing several methods can be used to approximate the time varying celerity. These methods generally consist of determining the celerity based on the averages of flow at two or three of the remaining grid points or by using an iterative procedure on all four grid points using a three point average as an initial estimate. All of these methods produce reasonable results and are quite simple to perform (Ponce and Theurer, 1982). However, this procedure requires that values of the parameters be determined for each time and space step which results in a great increase in computational effort. By routing various flow sequences with constant parameters and comparing these to the results of routing with variable parameters it has been found that choosing a reasonable value of a constant reference discharge will yield acceptable results (Ponce and Yevjevich, 1978). The celerity should be determined from a flood of record that is in the same size range of those that are to be routed. For the proposed state space formulation holding values of K and X to be constant for a reach greatly simplifies the computations required. In an irrigation system, the water is required during the low flow period of the year and large flood waves are unlikely. Therefore it should be possible to take a 'typical' summer flow and

determine the celerity for use in determining K and X. If it is desired to do some sort of flood study at a later time it would be advisable to choose a reference discharge that is similar to the normal flows that are found in the time period that flooding is of importance.

Discrete State Space Derivation

Due to the form of the river routing problem and the requirement that flows at intermediate points along the river are required, state space analysis is employed. State space is an n-dimensional space in which each axis represents one of the n state variables. The state of the system at any given time is expressed by the state variables. State space analysis is an analytical technique frequently used in modern control theory to solve sets of coupled or high order differential equations. It has several advantages over classical methods. State space analysis is accomplished in the time domain, it applies to problems with multiple inputs and outputs, and it includes the initial conditions. The classical theory operates in the frequency domain, has only a single input and output, and neglects the initial conditions. For these reasons a state space approach is used to solve the river routing problem. The Muskingum routing approach is written in terms of discrete time periods rather than in the form of differential equations as normally used in state space analysis, this required the development of a discrete state space solution for this set of difference equations.

The discrete state space formulation is written as:

$$F[\underline{x}(t)] = \underline{A}\underline{x}(t) + \underline{B}\underline{r}(t) \qquad 3.20$$

where:

F - the forward shift operator
$\underline{x}(t)$ - state vector
$\underline{r}(t)$ - the input vector (forcing function)
$\underline{A}$ - coefficient matrix
$\underline{B}$ - coefficient matrix

Solving for the Homogeneous Case. To find the solution of the equation one must first define the state transition matrix $\Phi(t)$ which gives the free response of the system such that:

$$\underline{x}(t) = \underline{\Phi}(t)\underline{x}(0)$$

To find the state transition matrix, start with the homogeneous equation

$$F[\underline{x}(t)] = \underline{A}\underline{x}(t)$$

or $$\underline{x}(t+1) = \underline{A}\underline{x}(t)$$

Taking Z transforms of this equation gives:

$$Z[\underline{x}(t+1)] = Z[\underline{A}\underline{x}(t)]$$

Expanding one obtains:

$$z\underline{X} - z\underline{x}(0) = \underline{A}\underline{X}$$

where $\underline{X} = Z(\underline{x})$

rearranging this gives

$$\underline{X} = (\underline{I} - \underline{A}/z)^{-1}\, x(0)$$

Then taking inverse Z transforms results in the solution:

$$\underline{x}(t) = Z^{-1}\,[(\underline{I} - \underline{A}/z)^{-1}]\,\underline{x}(0)$$

Thus the state transition matrix is:

$$\underline{\phi}(t) = Z^{-1}[(\underline{I} - \underline{A}/z)^{-1}] \qquad 3.21$$

which provides the unforced response to a vector of initial conditions.

Solving for the Non-Homogeneous Case. The non-homogeneous case includes the forcing function r(t) and the corresponding coefficient matrix B.

$$F[\underline{x}(t)] = \underline{A}\underline{x}(t) + \underline{B}\underline{r}(t)$$

Again, taking Z transforms of Eq. 3.20 gives:

$$z\underline{X} - z\underline{x}(0) = \underline{A}\underline{X} + \underline{B}\underline{R}(z)$$

where $\underline{R}(z) = Z[\underline{r}(t)]$

Rearranging one obtains:

$$\underline{X} = (\underline{I}-\underline{A}/z)^{-1}\ \underline{x}(0) + (\underline{I} - \underline{A}/z)^{-1}\ \underline{B}\underline{R}(z)/z$$

Again taking inverse Z transforms:

$\underline{x}(t) = Z^{-1}[(\underline{I} - \underline{A}/z)^{-1}]\ \underline{x}\ (0) + Z^{-1}\ [(\underline{I} - \underline{A}/z)^{-1}\ \underline{B}\underline{R}(z)/z]$ from the homogeneous solution of Eq. 3.20.

$$Z^{-1}\ [(\underline{I} - \underline{A}/z)^{-1}] = \underline{\phi}(t)$$

so, the solutions to the nonhomogeneous case is:

$$\underline{x}(t) = \underline{\phi}(t)\ x\ (0) + Z^{-1}[(\underline{I} - \underline{A}/z)^{-1}\ \underline{B}\underline{R}(z)/z]$$

To determine the inverse transform of $Z[(\underline{I} - \underline{A}/z)^{-1}\ \underline{B}\underline{R}(z)/z]$ the convolution property is used.

$$Z[f*g] = Z[f] * Z[g]$$

by letting

$$Z[f] = (\underline{I} - \underline{A}/z)^{-1}$$

and $Z[g] = \underline{B}\underline{R}(z)/z$

we obtain:

$$Z^{-1}\{Z[f]*Z[g]\} = Z^{-1}\{Z[f*g]\}$$

$$= f * g$$

so:

$$f = Z^{-1}[(\underline{I} - \underline{A}/z)^{-1}]$$

$$= \underline{\phi}(t)$$

$$g = Z^{-1}[\underline{BR}(t)/z]$$

$$= \underline{Br}(t) \text{ for instantaneous values of } r(t)$$

The convolution of f with g is defined as:

$$f * g = \sum_{k=0}^{h} f(k\Delta t)\ g[(h-k)\Delta t]$$

The complete solution of the discrete difference equation is then:

$$\underline{x}(t) = \underline{\phi}(t)\ \underline{x}(0) + \sum_{k=0}^{n} \underline{\phi}(k\Delta t)\underline{Br}[(h - k)\Delta t)] \qquad 3.21$$

Using this method it is possible to determine the response at any time given the input function r(t). If a continuous function is used to represent for the input r(t), a dirac delta function would need to be incorporated and would be obtained in taking the inverse Z transforms of equation above. The dirac delta function would sample the input vector at each of the discrete time steps thus reducing the continuous function to a set of discrete points. In this case, however, the input is defined to be a constant value for each time period thus eliminating the need for the delta function. For the proposed Muskingum routing, inputs consist of the inflow at the top of the reachs as well as the lateral inflows and diversions. Average values of these over the time increment Δt are used in the computations.

In the original form of the equation for multiple reaches exact results may be obtained by numerical methods, however, due to the

recursive nature, a solution at all intermediate time steps is required to get one answer at the desired time in the future. The discrete state space solution allows for the results to be solved for at any time in the future given the initial conditions and the inputs for each time step.

State Space Muskingum Routing

Recalling that the Muskingum routing method for a multiple reach system is:

$$Q_{j+1}^{n+1} = C_1 Q_j^n + C_2 Q_j^{n+1} + C_3 Q_{j+1}^n \qquad 3.13$$

In discrete state space notation, using constant parameters, this system of equations becomes:

$$F[\underline{Q}(t)] = \underline{A}\ \underline{Q}(t) + \underline{B}\ \underline{I}(t)$$

Specifically for this case:

$\underline{Q}(t)$ - flow in the reaches at time t

$\underline{I}(t)$ - inflow at the top of the uppermost reaches or lateral inflows to the other reaches

The elements of the A and B matrices are found by solving Eq. 3.13 for each reach and substituting so that each reach is defined in terms of all of the reaches above it. The notation of Eq. 3.21 is simple in vector form but is rather cumbersome when each element is expressed for use with Muskingum routing. This is due to the form of the input I(t), which actually consists of values of inflow at both time t and time t+1. This results in a $\underline{B}$ matrix with dimensions that are N by 2N for an N reach system. One way to simplify the $\underline{B}$ matrix, is to express it as two matrices, B1 and B2. This requires some minor changes in the solution.

Rewriting Eq. 3.21 as follows produces relatively simple expressions for the elements of the B matrix and will have no effect on the A matrix.

$$F[\underline{Q}(t)] = \underline{A}\ \underline{Q}(t) + \underline{B1}\ \underline{I}(t) + \underline{B2}\ \underline{I}(t+1) \qquad 3.23$$

where:

$\underline{B1}$ - coefficient matrix

$\underline{B2}$ - coefficient matrix

$\underline{I}(t)$ - known inflows to reaches at time t

$\underline{I}(t+1)$ - known inflows to reaches at time t+1

The solution using this formulation is written as:

$$\underline{Q}(t) = \underline{\phi}(t)Q(0) + \sum_{k=0}^{n} \underline{\phi}(kt)\underline{B1}\underline{I}[(h-k)\Delta t] + \underline{\phi}(kt)\underline{B2}\underline{I}[(h-k)\Delta t + \Delta t] \qquad 3.24$$

For an N reach non-branching system the elements of the $\underline{A}$ matrix as determined from Eq. 3.13, where i represents the row of the element, k represents the column, and L is a counter.

For $i < k$ $\quad a(i,k) = 0$

For $i = k$ $\quad a(i,k) = C_{i,3}$

For $i = k+1$ $\quad a(i,k) = [C_{k+1,1} + C_{k+1,2}\ C_{k,3}]$

For $i > k+1$ $\quad a(i,k) = \left[\prod_{L=k+2}^{n} C_{L,2}\right]\left[C_{k+1,1} + C_{k+1,1}\ C_{k,3}\right]$

With the same notation, the elements of the B1 and B2 matrices are:

For $i < k$ $\quad b1(i,k) = 0$ $\qquad b2(i,k) = 0$

For $i = k$ $\quad b1(i,k) = C_{i,1}$ $\qquad b2(i,k) = C_{i,2}$

For $i > k$ $\quad b1(i,k) = \left[\prod_{L=k+1}^{n} C_{K,2}\right] C_{k,1}$

For $i > k$ $\quad B2(i,k) = \left[\prod_{L=k+1}^{n} C_{K,2}\right] C_{k,2}$

Recalling that the state transition matrix is determined by Eq. 3.21, general expressions for terms of $\phi(t)$ can be found but are algebraically very complex and cumbersome. To illustrate this, the state transition matrix of a three reach system with no lateral inflow is determined. The elements of the A matrix are determined from Eq. 3.13 above to be:

$$\underline{A} = \begin{bmatrix} C_{1,3} & 0 & 0 \\ C_{2,1} + C_{2,2} + C_{1,3} & C_{2,3} & 0 \\ C_{3,2}[C_{2,1} + C_{2,2} + C_{1,3}] & C_{3,1} + C_{3,2} + C_{2,3} & C_{3,3} \end{bmatrix}$$

Letting the elements of the A matrix be represented as a(i,j), where i represents the row and j the column, the elements of the state transition matrix can be determined from the following equations.

For $i < j$ $\quad \underline{\phi}(i,j) = 0$

For $i = j$ $\quad \underline{\phi}(i,j) = a(i,i)$

For $i = j+1$ $\quad \underline{\phi}(i,j) = a(i,j) \dfrac{a(i,i)}{(a(i,i) - a(j,j))} + \dfrac{a(j,j)}{(a(j,j) - a(i,i))}$

For $i = j+2$

$$\underline{\phi}(i,j) = a(i-1,i-2)a(i,i-1) \frac{a(i-1,i-1)}{(a(i-1,i-1)-a(i-2,i-2))(a(i-1,i-1)-a(i-3,i-3))} + \frac{a(i-2,i-2)}{(a(i-2,i-2)-a(i-1,i-1))(a(i-2,i-2)-a(i-3,i-3))} + \frac{a(i-3,i-3)}{(a(i-3,i-3)-a(i-2,i-2))(a(i-3,i-3)-a(i-1,i-1))} + a(i,j) \frac{a(i-1,i-1)}{a(i-1,i-1)-a(i,i)} + \frac{a(i-1,j-1)}{(a(i,i) - a(i-1,i-1)}$$

This simple example clearly demonstrates how the terms of the matrix become very complex when written in general terms of t. The complexity of these equations increases geometrically as the number of reaches increases and becomes very cumbersome even for a simple system. An alternative to solving for a general, time varying, transition matrix is to use a one step ahead transition matrix with the outflows at one time period as the initial conditions for the next. The A matrix is a one step ahead transition matrix as can be verified by setting t equal to one in the above equations or simply by the form of the initial equation. This method is much less cumbersome as can be seen by comparing the elements of the A matrix to the elements of the matrix.

SOIL MOISTURE

The movement of water into and through the zone in which plants can extract moisture is a complex phenomenon. It involves infiltration, redistribution of the water within the root zone, drainage from the root zone, evaporation and transpiration. These processes are very important as they affect the amount of water that is required for irrigation. Models that accurately describe these phenomena can be used to determine the timing and amount of irrigation that a crop requires. Such knowledge is crucial to an irrigation management system.

This section presents a brief description of the processes involved in moisture depletion. The simplified soil moisture model

given by Koch and Allen (1985) is presented and developed into a form to facilitate sensitivity and error analysis. The results of this are used to determine the errors associated with irrigation demands which are then tracked through the streamflow routing model.

Moisture Transport in Soil

To explain transport in soil several definitions are required. Soil moisture is defined as the ratio of the volume of water to the bulk volume of soil. The field capacity, θ_{fc}, is the soil moisture below which no loss due to gravity drainage occurs. The wilting point, $O_{\omega p}$, is the soil moisture at which a plant can no longer extract water from the soil. Natural saturation, θ_s, is the soil moisture at which the voids are nearly full of water. This is usually less than the porosity of the soil as there is often trapped air within the soil. The root zone is the depth to which plants can extract water from the soil.

The processes involved in moisture transport in soil include infiltration, redistribution, percolation, evaporation, and transpiration. Infiltration is the transport of moisture into the soil surface. Redistribution occurs following a precipitation or irrigation and causes the soil moisture to even out throughout the soil column. This process occurs rather rapidly following an irrigation or precipitation event. Drainage is the process of water draining from the root zone by gravity following the redistribution of an irrigaton or precipitation. This tends to be a rather slow process and occurs when the soil moisture is in excess of field capacity. The

major factors affecting redistribution and drainage are the hydraulic conductivity and the capillary pressure properties of the soil. Evaporation is the loss of moisture from the soil surface to the atmosphere and transpiration is the removal of moisture from the soil by the plants. These two processes have very similar characteristics and are often modeled together (Saxton and McGuinness, 1982). Collectively the process is referred to as evapotranspiration (ET). The two major factors controlling ET are energy inputs, such as sensible heat and solar radiation, and the availability of water in the soil.

The combination of these processes lead to complex nonlinear differential equations for which there is no analytical solution. Simplifications, numerical methods, or both are needed to solve these problems for practical applications.

Simplified Soil Moisture Model

The soil moisture model presented by Koch and Allen (1985) describes the movement of water through the root zone and the moisture depletion due to ET. Many simplifying assumptions were made to obtain this model yet the parameters are still physically measureable and the results seem to be adequate. For the ET phase the model is written as:

$$\theta(t) = \theta wp + (\theta o - \theta wp)\exp[-ET_p\, t/[D(\theta fc - \theta wp)] \qquad 3.24$$

where: $\theta(t)$ - soil moisture at time t
θo - soil moisture at time 0
ET_p - potential evapotranspiration
D - depth of root zone

In this application, only the ET process is modeled which restricts the applicability to areas where irrigation methods are efficient and no excess water is applied which result in drainage. The major assumptions made in this model are:

1. Redistribution occurs rapidly with respect to ET so no separate calculations for redistribution are needed.

2. ET is assumed to be a linear function of the soil moisture, starting at zero when θ = o and reaching the potential rate of ET (PET) when θ > o.

3. This model is only adequate for situations in which the soil moisture is at or below field capacity following redistribution.

The model is inappropriate under conditions where θ > o since drainage from the root zone is not considered. This study addresses only the model presented which limits applicability to relatively efficient methods of irrigation that will apply no excess water. For soil moisture greater than θ, in which drainage occurs, additional components are available (Koch and Allen, 1985).

PET is modeled using the Jensen-Haise equation, an empirical relationship between PET, temperature, and solar radiation. It is as follows:

$$ET_p = (9.1598 * 10^{-6} T - 2.4167 * 10^{-4})R_s \qquad 3.25$$

where:

ET_p - potential evapotranspiration in inches per day
T - average temperature in degrees fahrenheit
R_s - 24 hour solar radiation total in Langleys per day

Rewriting Eq. 3.24 in terms of available water gives:

$$AWC(t) - AWC(0) \exp[-ETp\ t/(AW\ D)] \qquad 3.26$$

where:

AWC(t) - available water at time t ($\theta(t) - \theta wp$)
AWC(0) - initial available water ($\theta(0) - \theta wp$)
AW - total available water ($\theta fc - \theta wp$)

Adding a forcing function such as rainfall or an irrigation, and a term representing model error, the model becomes:

$$AWC(t) = AWC(0) \exp[-ET_p \, t/(AW \, D)] + r(t)/D + w(t) \qquad 3.27$$

where:
r(t) - input, precipitation or irrigation
w(t) - model error

This formulation is valid for an input r(t) such that $0 + r(t)/d < 0$ based on the restricted applicability of the model. This formulation can be readily analyzed for sensitivity and error propagation.

The parameters of this model are estimated from the physical characteristics of the system. The complete model has been used to describe soil moisture in the Tualatin Valley Irrigation District. Results indicate an adequate reproduction of observed soil moisture given the required climatological data from the historic record (Allen 1985).

The results of this model, when used to forecast, determine the amount of water that is required for irrigation as well as the timing of the irrigation based on crop needs. When adjusted for irrigated area, the resulting diversion is an input to the river routing model which is used to determine whether demands can be met. Other factors to consider when irrigating include soil contamination by inorganic salts and irrigation efficiency. Soil contamination may dictate that

more water than required for plant growth be supplied in order to wash the salts from the soil. This is not considered in the soil moisture model presented here but may be important in certain situations. In addition, the actual amount of water that reaches the ground is less than the water that is removed from the river system. Losses from conveyance and from the actual application of the water can vary considerably with the methods being used as well as the climatic conditions. This is considered in determining the amount of diversion required.

CHAPTER IV

SENSITIVITY, FORECAST ERRORS, AND ERROR PROPAGATION

One of the major objectives of this study is the evaluation of forecast errors and the determination of how errors propagate through the system. The ability to determine the sensitivity of the model to the various inputs, throughout the system from soil moisture demand to the source of water, is of great aid in determining the utility of the models. Such an analysis provides an objective means by which to measure the relative effects of forecast errors. This, in turn, suggests where effort must be centered in constructing forecast models. It is desirable to improve the parts of the model that yield the greatest increase in model performance. These can be identified using a sensitivity analysis and tracking errors through the system. In a model such as this where the results of one component or reach are used as the input for the next component or reach, any error in the input will propagate through all lower segments of the model. A determination of what happens to these errors is necessary to determine whether the model will provide reasonable results. It is possible that the errors could grow unbounded or just grow until they reach a constant value. Even if the errors were to grow unbounded they may grow slowly enough at first so that their effects are not significant within the time frame that the forecasts are needed. With

an analysis of error propagation it is possible to objectively determine how the errors behave.

TEMPERATURE AND SOLAR RADIATION FORECAST ERRORS

The model chosen to forecast temperature and solar radiation is a multivariate autoregressive model (MVAR). The form of this model is:

$$\underline{z}(v,t) = \underline{A}(t)\ \underline{z}(v,t-1) + \underline{B}(t)\underline{\varepsilon}(v,t) \qquad 4.1$$

with terms as defined in chapter 2. For ease of forecast error development, this model can be written in single variate form as:

$$\underline{z}(t+1) = [\underline{A}\underline{z}(t) + \underline{B}(t)\underline{\varepsilon}(t)] \qquad 4.2$$

Or, the model may be written in terms of the lead time, L, as:

$$\underline{z}(t+L) = \underline{A}^{L}\underline{z}(t) + \underline{A}^{L-1}\underline{B\varepsilon}(t+1) + \ldots + \underline{AB\varepsilon}(t+L-1) \qquad 4.3$$

By taking the term by term expectation the forecast function is found.

$$\underline{z}(L) = \underline{A}^{L}\underline{z}(t) \qquad 4.4$$

The forecast error at lead time L is the difference between the actual value and the forecast value and is written as:

$$\underline{e}(L) = [\underline{z}(t+L) - \underline{z}(L)] \qquad 4.5$$

where:

$\underline{e}(L)$ - forecast error at lead time L
$\underline{z}(t+L)$ - actual value
$\underline{z}(L)$ - forecast value

Substituting Eq. 4.3 and 4.4 into Eq. 4.5, an expression for the error at lead time L is obtained.

$$e(L) = A^{L-1}B\varepsilon(t+1) + \ldots + AB\varepsilon(t+L-1) + B\varepsilon(t+1) \qquad 4.6$$

with variance determined by:

$$VAR[\underline{e}(L)] = E[\underline{e}(L)\underline{e}(L)^T] \tag{4.7}$$

$$= E[\underline{A}^{L-1}\underline{B\varepsilon}(t+1) + \ldots + \underline{AB\varepsilon}(t+L-1) + \underline{B\varepsilon}(t+1))$$

$$(\underline{A}^{L-1}\underline{B\varepsilon}(t+1) + \ldots + \underline{AB\varepsilon}(t+L-1) + \underline{B\varepsilon}(t+1))^T]$$

Expanding equation 4.7 and recalling that the noise terms are uncorrelated leads to a general expression for the forecast error covariance at lead time, L, given by:

$$E[e(L)e(L)^T] = [A^{L-1}BB(A^{L-1})^T + \ldots + ABB^TA^T + BB^T] \tag{4.8}$$

ARMA FORECASTING MODEL ERROR

An ARMA model of orders p and q has the form:

$$z(t) = \sum_{i=1}^{p} \phi_i Z(t-1) + \varepsilon(t) - \sum_{j=1}^{q} \theta_j \varepsilon(t-j) \tag{4.9}$$

with terms as defined in chapter 2.

or

$$\sum_{i=0}^{p} \phi_i z(t-j) - \sum_{j=0}^{q} \phi_j \varepsilon_{t-j} = 0 \tag{4.10}$$

This model can also be written as the infinite sum of weighted independent random variables.

$$z(t) = \sum_{j=0}^{\infty} \Psi_j \varepsilon_{t-j} \tag{4.11}$$

where:

Ψ_j - weighting factors

Forecast errors can be expressed as:

$$e(L) = \sum_{j=0}^{L-1} \Psi_j \epsilon_{t+L-j} \qquad 4.12$$

where:

e(L) - forecast error at lead time L

(Salas et al., 1980). Substituting Eq. 4.14 into Eq. 4.15 one obtains:

$$\sum_{j=0}^{p} \sum_{i=0}^{\infty} \theta_j \Psi_j \epsilon_{t-j-1} - \sum_{j=0}^{q} \theta_j \epsilon_{t-j} \qquad 4.13$$

To determine the variance of the forecast error, the Ψ terms must be found. This can be done by solving Eq. 4.13 recursively. For an AR(p) model the Ψ terms are:

$$\Psi_j = \sum_{i=1}^{p} \phi_i \Psi_{j-i} \qquad 4.14$$

where:

$\Psi_o = 1$

$\Psi_{j-1} = 0$ where $j - 1 < 0$

For an ARMA(1,1) model the terms are:

$$\Psi_j = (\phi_1 - \theta_1)\phi_1^{j-1} \qquad 4.15$$

With the Ψ terms known, the variance of the forecast error can then be determined.

$$\mathrm{Var}[e(L)] = E[e^2(L)] \qquad 4.16$$

$$= \sum_{j=0}^{L-1} \Psi_j^2 \sigma_\epsilon^2$$

The variance of the forecast error for a one step ahead forecast is the residual variance of the model. As the lead time increases the error variance approaches the variance of the system modeled.

SENSITIVITY ANALYSIS

To determine the sensitivity of the soil moisture model to the parameters and forecasts of input variables (temperature and solar radiation), it is necessary to perform a sensitivity analysis. This is accomplished by determining the contribution that each of the parameters and forecasts makes to the variance of the modeled variable. The approximate variance of the result can be determined from the first order Taylor series approximation, which is given by:

$$\sigma^2 = (\partial R/\partial x_1 \ \sigma x_1)^2 + (\partial R/\partial x_2 \ \sigma x_2)^2 + \cdots + (\partial Rn/\partial xn \ \sigma xn)^2 \qquad 4.17$$

where:

R - is the function under evaluation

X_i - parameters or forecast variables

n - number of parameters and/or forecast variables

Recalling the form of the soil moisture model:

$$AW(t) = AW(0) \exp-[ET_p/D \ AWC]$$

where:

$$ET_p = (9.1598*10^{-6}T - 2.4167*10^{-4})Rs$$

with terms as defined in Chapter 3. To estimate the sensitivity or variance of soil moisture to the parameters and the forecasts for temperature and solar radiation the following equation can be applied:

$$\sigma^2_{AW} = (\partial AW(t)/\partial AW(0) \ \sigma_{AW(0)})^2 + \partial AW(t)/\partial AWC \ \sigma_{AWC})^2 + (\partial AW(t)/\partial T \ \sigma_T)^2 + (\partial AW(t)/\partial R_s \ \sigma_{Rs})^2 + (\partial AW(t)/\partial D \ \sigma_D)^2 \qquad 4.18$$

However, the variance of the parameters is not known and cannot easily be determined, thus the analysis can only provide relative sensitivities for the parameters using the coefficients of Eq. 4.18 as a guide. The parameters, in this case, are physically measureable

quantities. The variance of these measurements are dependent on such considerations as the skill of the person performing the measurement, the precision of the instrument or method used to develop the data, and the natural variability that exists in the variable being analyzed.

Since the forecast error variance can be determined, estimated values for the variance of soil moisture with respect to temperature and solar radiation can be obtained as:

$$\sigma^2_{AW} = (\partial AW(t)/\partial t\ \sigma_T)^2 + (\partial AW(t)/\partial R_S\ \sigma_{R_S})^2 + \left(\frac{\partial AW}{\partial AW(i)}\ \sigma_{AW(i)}\right)^2$$

$$= \left[AW(i)\ \exp -\left[\left[\frac{9.1598 \times 10^{-6}T - 2.4167 \times 10^{-4}}{D \times AWC}\right]R_S(i)\right] \times \frac{9.1598 \times 10^{-6}(R_S(i)}{D \times AWC}\ \sigma_T\right]^2 +$$

$$\left[AW(i)\ \exp -\left[\left[\frac{9.1598 \times 10^{-6}T - 2.4167 \times 10^{-4}}{D \times AWC}\right]R_S(1)\right] \times \left[\frac{9.1598 \times 10^{-6}T - 2.4167 \times 10^{-4}}{D \times AWC}\right]\sigma_{R_S}\right]^2 +$$

$$\left[\exp -\left[\left[\frac{9.1598 \times 10^{-6}T - 2.4167 \times 10^{-4}}{D \times AWC}\right]R_S\right]\sigma_{AW(i)}\right]^2$$

which provides the forecast error variance of the soil moisture assuming that the parameters are perfect.

ERROR PROPAGATION

Errors are introduced through all the models presented. The results of the climate forecasting models are used as input to the soil moisture model. These results as well as streamflow forecasting are used as input to the routing model. The routing model indicates whether there is adequate water for irrigation. thus, all of the models presented are interrelated. Unfortunately, the errors of each of the models are interconnected as well. This section presents a method to track propagation of errors through the system.

The following error propagation analysis (Gelb 1974) is presented using the state space notation of chapter 3 primarily for its incorporation with the discrete Muskingum state space solution. This technique is used with the soil moisture model as well, when reduced to a scalar rather than vector form. The following definitions are presented to provide the required background. The state of a system whose output is X can be written as:

$$\underline{x}(t+1) = \underline{\phi}(t)\underline{x}(t) + \underline{\Gamma}(t)\underline{w}(t) + \underline{\Lambda}(t)\underline{u}(t) + \underline{\kappa}(t)\underline{v}(t) \qquad 4.20$$

where:

$\underline{\phi}(t)$ - state transition matrix as described in chapter 2

$\underline{\Gamma}(t)$ - a convolution matrix as described in chapter 2 representing the model error coefficients

$\underline{w}(t)$ - model error at time t

$\underline{\Lambda}(t)$ - convolution matrix for "known" model input

$\underline{u}(t)$ - known model input

$\underline{\kappa}(t)$ - convolution matrix for input errors

$\underline{v}(t)$ - errors of the input

In this analysis the coefficient matrices are assumed to be constant. The error covariance matrix, P(t), at time t is defined as:

$$\underline{P}(t) = E[\underline{\tilde{x}}(t)\underline{\tilde{x}}(t)^T] \qquad 4.21$$

where:

E - the expected value operator

$\underline{\tilde{x}}(t)$ - error vector, $\underline{\hat{X}}(t) - \underline{X}(t)$ 4.22

$\underline{x}(t)$ - observed value vector

$\underline{\hat{x}}(t)$ - estimated value vector

Substituting Eq. 4.24 into Eq. 4.26 one obtains:

$$\underline{\hat{x}}(t+1) - \underline{x}(t+1) = \underline{\phi}(t)\underline{\hat{x}}(t) - [\underline{\phi}(t)\underline{x}(t) + \underline{\Gamma}(t)\underline{w}(t)$$

$$+ \underline{\lambda}(t)\underline{u}(t) + \underline{\kappa}(t)\underline{v}(t)]$$

Note that the term $\underline{\Lambda}(t)\underline{u}(t)$ is a known input and introduces error into the system.

From this:

$$\underline{\hat{x}}(t+1) = \underline{\phi}(t)\underline{\hat{x}}(t) - \underline{\Gamma}(t)\underline{w}(t) - \underline{\kappa}(t)\underline{v}(t) \qquad 4.23$$

So the error covariance matrix at time t+1 is:

$$P(t+1) = E[(\underline{\phi}(t)\underline{\tilde{x}}(t)\underline{\tilde{x}}(t)^T\underline{\phi}^T(t) - \qquad 4.24$$

$$\underline{\phi}(t)\underline{\tilde{x}}(t)\underline{w}(t)^T\underline{\Gamma}(t)^T + \underline{\phi}(t)\underline{\tilde{x}}(t)\underline{v}(t)^T\underline{\kappa}(t)^T -$$

$$\underline{\Gamma}(t)\underline{w}(t)\underline{\tilde{x}}(t)^T\underline{\phi}^T(t) + \underline{\Gamma}(t)\underline{w}(t)\underline{w}(t)^T\underline{\Gamma}^T(t) +$$

$$\underline{\Gamma}(t)\underline{w}(t)\underline{v}(t)^T\underline{\kappa}^T(t) - \underline{\kappa}(t)\underline{v}(t)\underline{\tilde{x}}(t)^T\underline{\phi}^T(t) +$$

$$\underline{\kappa}(t)\underline{v}(t)\underline{w}(t)^T\underline{\Gamma}^T(t) + \underline{\kappa}(t)\underline{v}(t)\underline{v}(t)^T\underline{\kappa}^T(t)]$$

For the terms in which the random variables are not the same, the expected value is zero since these errors are uncorrelated. For example:

$$E[x(t)(\Gamma(t)w(t))^T] = 0$$

Thus, Eq. 4.6 reduces to:

$$P(t+1) = E[\underline{\phi}(t)\underline{\tilde{x}}(t)\underline{\tilde{x}}(t)^T\underline{\phi}^T(t)] + E[\underline{\Gamma}(t)\underline{w}(t)\underline{w}(t)^T\underline{\Gamma}^T(t)] + E[\underline{\kappa}(t)\underline{v}(t)\underline{v}(t)^T\underline{\kappa}(t)^T] \quad 4.25$$

which becomes:

$$P(t+1) = \underline{\phi}(t)\underline{P}(t)\underline{\phi}^T(t) + \underline{\Gamma}(t)R(t)\underline{\Gamma}^T(t) + \underline{\kappa}(t)\underline{S}(t)\underline{\kappa}^T(t) \quad 4.26$$

where:

$\underline{R}(t)$ - covariance matrix of the model error

$\underline{S}(t)$ - covariance matrix of the input error

Using equation 4.8 the error covariance matrix at time period t+1 can be found from the error covariance matrix at the time t with the model and input error covariance matrices.

It is interesting to note the Eq. 4.26 is a difference equation from which a general solution could be obtained. This could be useful for further investigation of error propagation, but would most likely become computationally cumbersome as did the general solution to the Muskingum routing problem of chapter 3.

CHAPTER V

APPLICATION OF FORECAST MODELS

To demonstrate the fitting, use, and forecast error variance of each of the selected models, numerical examples are provided using data from the Tualatin Valley Irrigation District (TVID) and the U.S. Geological Survey. Each of the models are fit and analyzed for forecast error variance with examples showing the individual model response. Following this, an example is given for a simplification of the entire system using all of the component models. The error variance associated with each model is calculated and the forecast error variance is determined for the entire system.

The Tualatin River Basin is chosen as the study area for these examples because it is typical of a small river basin in Western Oregon and is one of the few areas where most of the data required to fit and test these models are available due to the activities of the TVID. This area is especially useful because of its relatively long, five year, record of solar radiation. A map of the basin and the surrounding area is shown in Figure 5. To simplify computations, water users are consolidated into five major diversions in the examples. This simplifies computations but still adequately demonstrates the models. Because most of the required data is available, few further modifications are required.

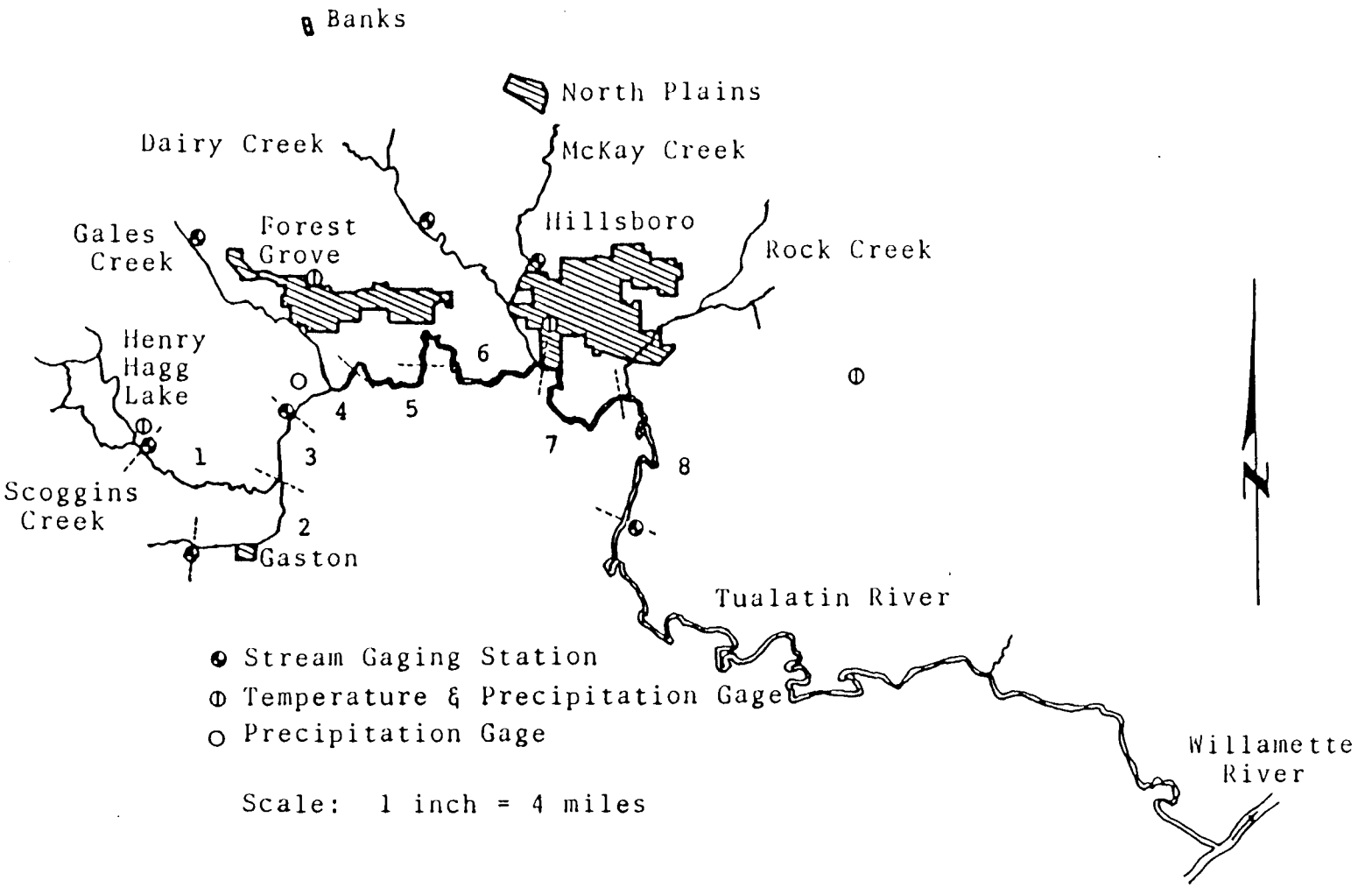

Figure 5 Map of the Tualatin River study area. Numbers indicate river reach.

WEATHER FORECASTING

Precipitation

To determine the characteristics of the precipitation occurrence and quantity of the Tualatin Valley, a Markov chain analysis was performed on a 29 year climatological data set from 1952-1981 from Forest Grove, Oregon. Analysis indicated that seven states adequately discretize the data. To accommodate periodicity, the data are grouped into 14 day periods. To demonstrate typical forecast development, the transition occurrences and probabilities as well as the forecast values are determined for the two week period beginning July 22 and ending August 4. These values are shown in Tables III and IV respectively. The transition probabilities for the other period are listed in the Appendix. They show that the most common transition is the no rain to no rain situation. The forecasts demonstrate that even in the event that it does rain there is little rain on the following day. For example, if on day 0 there was .25 inches of rain, the forecast for day 1 would be for 0.125 inches. The forecast for day 2 would then be 0.01 inches and for the following days, the forecast would be zero inches of rain.

Temperature and Solar Radiation

For the Tualatin River basin a five year solar radiation record, available from the TVID, was used with the associated temperature and precipitation record to fit the MVAR model. These data included daily high and low temperatures as well as cumulative solar radiation. Mean

TABLE III

PRECIPITATION TRANSITION FREQUENCIES

	State on Day t+1							
State on Day t	1	2	3	4	5	6	7	SUM
1 (0.0 in.)	363	8	5	3	0	0	1	380
2 (.01-.05)	9	2	0	2	2	1	1	13
3 (.05-.10)	4	1	0	0	0	0	1	5
4 (.10-.15)	1	1	0	0	1	0	0	3
5 (.15-.20)	1	0	0	0	0	0	0	1
6 (.20-.25)	1	0	0	0	0	1	0	2
7 (> 0.25)	0	2	0	0	0	0	0	2

TABLE IV

TRANSITION PROBABILITIES
AND FORECAST VALUES

	State on Day t+1							
State on day t	1	2	3	4	5	6	7	FORECAST
1 (0.0 in.)	.955	.021	.013	.008	0	0	0	.0051
2 (.01-.05)	.692	.154	0	0	0	.077	.077	.0655
3 (.05-.10)	.800	.200	0	0	0	0	0	.0100
4 (.10-.15)	.333	.333	0	0	.333	0	0	.0833
5 (.15-.20)	1.0	0	0	0	0	0	0	0.0
6 (.20-.25)	.500	0	0	0	0	.500	0	.1250
7 (> 0.25)	0	1.0	0	0	0	0	0	.0500

daily temperatures are assumed to be the arithmetic average of the high and low temperatures. The record for the solar radiation was not complete apparently because the cummulative solar radiation meter used was not read on weekends. This resulted in a solar radiation record that typically consisted of four days per week of daily readings followed by a cumulative reading for the remaining three days per week. To obtain a continuous set of daily data, as required by the model, it was necessary to synthesize values for the days that had no readings. This was accomplished by fitting a regression between the temperature and the solar radiation for the days on which solar radiation data was read. To accommodate periodicity a different regression was fit for each month. The best fits, for all periods, was obtained using a linear regression with daily high temperature as the regressor. Using the regression relations, estimates for the missing data were calculated from the temperature data. The cumulative radiation that was read over the period of missing data was then distributed in proportion to the estimated quantities that each of the days received from the regression. This procedure attempts to maintain the assumed relation between temperature and solar radiation while keeping the cumulative radiation of the missing data equal to the actual amount.

Using the five year data set, the parameters of the MVAR model were estimated. To accommodate periodicity an attempt was made to use daily means, standard deviation, and correlation coefficients; however, doing so produced some unrealistic negative correlations. Seven and 14 day periods were also tried. The 14 day period smoothed

the statistics well, showed good correlation and was chosen as the appropriate period length for mean and standard deviation. The correlation coefficients showed minimal periodicity and were recalculated for the entire period. These statistics are shown in Table V. Using these statistics, the A and B coefficient matrices were determined; they are shown in Table VI. From these, the error covariance matrices are determined; they are shown in Table VII. The diagonal terms of these matrices are the variance and are used to determine variance of the soil moisture model. These terms start off relatively small and increase towards one as the forecast lead time increases. This indicates that the forecasts obtained by this model are better than merely forecasting the mean, for a lead time of only a few days. As the lead time increases, the variance of the forecast approaches the sample variance. As this happens, the utility of the model decreases. With higher correlations, these variance terms would stay lower for longer periods thus providing better forecasts.

Sample forecasts are shown in figure 6 through 8 demonstrating the behavior of the model under different initial conditions. It is interesting to note that this model behaves quite differently from a simple single-variate AR(1) model. With an AR(1) model a forecast always directly approach the mean value. With the MVAR it is possible for forecast values to increase for a time period or two before approaching the mean and at a rate different from that which would occur in a single variate model. These forecasts tend to indicate that solar radiation is more strongly influenced by temperature than one might expect. This may be due to the manner in

TABLE V

TEMPERATURE AND SOLAR RADIATION STATISTICS

TEMPERATURE

Day	Dry Mean	Wet Mean	Dry Std. Dev.	Wet Std. Dev.
1-14	54.05	51.42	4.74	3.95
15-28	60.66	52.34	6.46	3.15
29-42	59.53	56.19	5.24	2.70
43-56	63.52	57.87	6.18	4.23
57-70	64.38	59.10	4.51	3.93
71-84	66.37	64.42	4.92	3.61
85-98	67.81	62.40	5.22	2.16
99-112	68.97	61.88	6.56	2.90
113-126	64.85	63.69	4.93	4.32
127-141	63.88	60.88	5.23	4.38
142-153	58.60	55.75	5.95	3.72

SOLAR RADIATION

Day	Dry Mean	Wet Mean	Dry Std. Dev.	Wet Std. Dev.
1-14	456.4	360.9	142.8	166.6
15-28	485.1	428.27	134.5	117.9
29-42	465.7	327.3	152.8	75.0
43-56	469.7	361.0	141.7	130.5
57-70	474.9	380.5	158.7	104.0
71-84	519.2	372.5	131.0	112.0
85-98	504.3	312.8	148.6	93.3
99-112	450.8	304.8	126.4	56.8
113-126	393.7	283.6	118.4	87.4
127-141	386.9	310.2	107.9	110.3
142-153	319.8	245.4	95.8	59.1

CORRELATION COEFFICIENTS

	Lag 0	Lag 1
Temperature - Temperature	1.0000	0.5978
Temperature - Solar Radiation	0.4904	0.4032
Solar Radiation - Solar Radiation	1.000	0.5420
Solar Radiation - Temperature	0.4904	0.1717

TABLE VI

A AND B PARAMETER MATRICES

$$A = \begin{bmatrix} 0.5268 & 0.1448 \\ 0.6027 & -0.1238 \end{bmatrix} \qquad B = \begin{bmatrix} 0.7916 & 0.0000 \\ 0.2274 & 0.8018 \end{bmatrix}$$

TABLE VII

RESIDUAL FORECAST ERROR VARIANCE MATRICES OF TEMPERATURE AND SOLAR RADIATION

Lead Time (Days)		Lead Time (Days)	
1	$\begin{bmatrix} .6267 & .1800 \\ .1800 & .6946 \end{bmatrix}$	5	$\begin{bmatrix} .9892 & .5126 \\ .5126 & .9926 \end{bmatrix}$
2	$\begin{bmatrix} .8426 & .3712 \\ .3712 & .9054 \end{bmatrix}$	6	$\begin{bmatrix} .9956 & .5176 \\ .5176 & .9966 \end{bmatrix}$
3	$\begin{bmatrix} .9360 & .4702 \\ .4702 & .9587 \end{bmatrix}$	7	$\begin{bmatrix} .9982 & .5197 \\ .5197 & .9982 \end{bmatrix}$
4	$\begin{bmatrix} .9736 & .5004 \\ .5004 & .9831 \end{bmatrix}$		

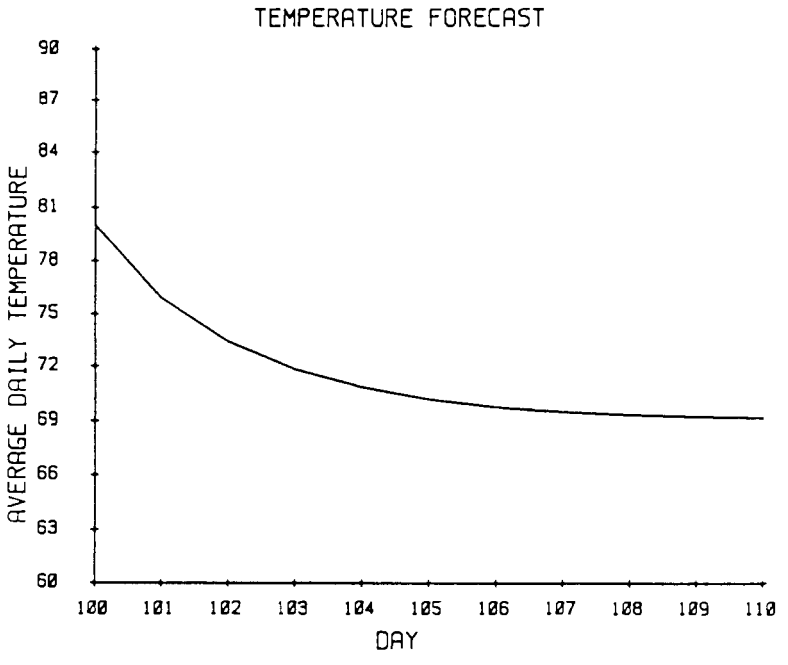

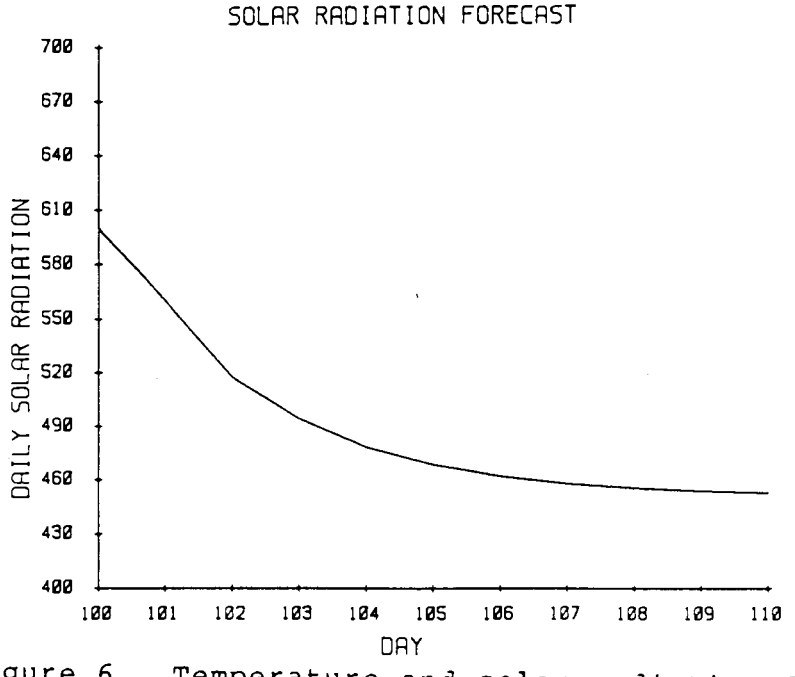

Figure 6. Temperature and solar radiation forecast with above average initial conditions.

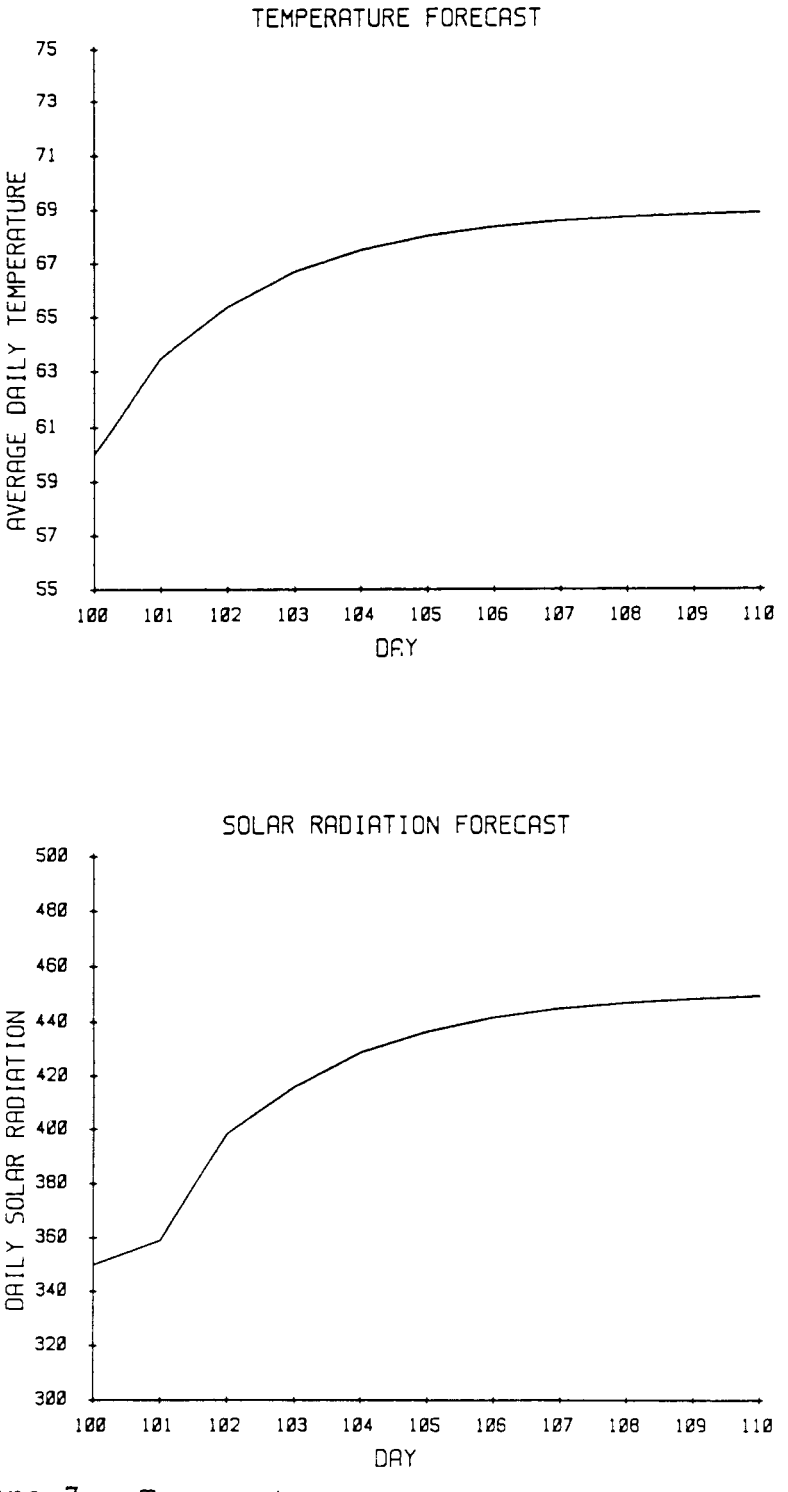

Figure 7. Temperature and solar radiation forecast with below average initial conditions.

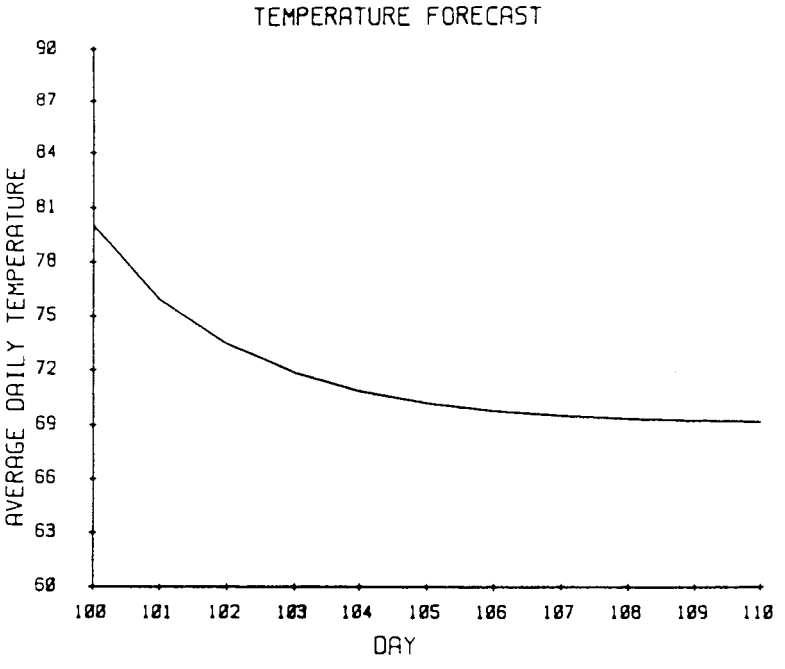

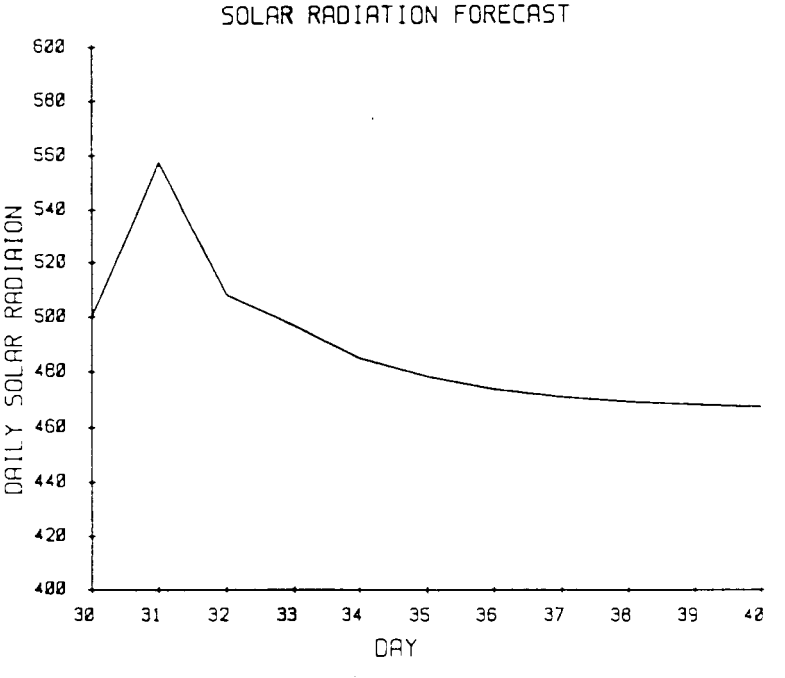

Figure 8. Temperature and solar radiation forecast with above average solar radiation and below average temperature initial conditions.

which the missing data was filled in for the solar radiation. However, the linear regression only preserved the lag zero correlation but did nothing to preserve the lag one correlation that would tend to make temperature follow solar radiation.

SOIL MOISTURE

To demonstrate the soil moisture model and the water demands that are derived from the results, the Tualatin Valley Irrigation District is simulated with only five major water users. This simplifies computation, but is adequate to demonstrate the behavior of the model and the errors associated with it. The pertinent information about each water user is provided in Table VIII. Irrigations are performed when the soil moisture drops below the critical soil moisture. The amount of water required is the difference between the field capacity and the soil moisture on the day of the irrigation multiplied by the number of acres and the root zone depth. This quantity is then assumed to be withdrawn evenly from the river over the entire day of the irrigation. The error variance of soil moisture is determined from Eq. 4.19. The variance of temperature and solar radiation, required in this equation, are determined from the diagonal terms of the residual forecast error variance of Table VII and are shown graphically in Figure 9. Table IX shows the normalized contributions of temperature, solar radiation, and initial available water to the overall variance of the model. The soil moisture error variance values generally increase as the forecast

TABLE VIII

WATER RIGHT INFORMATION
JULY 24 - 31, 1974

Field Number	1	2	3	4	5
Priority	1	2	3	4	5
Diversion Reach	8	4	8	6	1
Irrigated acres	800	450	350	80	180
Root Zone Depth	12	12	18	12	18
Critical soil moisture,	0.10	0.15	0.30	0.10	0.30
Field Capacity,	0.35	0.33	0.38	0.40	0.40
Wilting Point,	0.15	0.13	0.18	0.13	0.22
Initial Soil Moisture, (0)	0.30	0.30	0.22	0.35	0.26
Available water content, AWC	0.20	0.20	0.20	0.27	0.18
Critical avaliable water content, AW	0.0	0.02	0.12	0.0	0.08
Initial available water content, AW(0)	0.15	0.17	0.14	0.22	0.10

TABLE IX

NORMALIZED CONTRIBUTIONS OF FORECAST ERROR VARIANCE TO SOIL MOISTURE VARIANCE

	LEAD TIME (DAYS)						
	1	2	3	4	5	6	7
FIELD 1							
Temperature	.147	.079	.055	.043	.034	.028	.024
Solar Radiation	.853	.492	.315	.241	.191	.156	.132
Initial Soil Moisture	0.0	.429	.629	.715	.774	.816	.844
FIELD 2							
Temperature	.147	.080	.057	.043	.032	.027	.028
Solar Radiation	.853	.493	.323	.243	.180	.148	.125
Initial Soil Moisture	0.0	.428	.620	.714	.788	.826	.852
FIELD 3							
Temperature	.147	.079	.096	.060	.044	.034	.028
Solar Radiation	.853	.491	.544	.338	.244	.190	.156
Initial Soil Moisture	0.0	.429	.360	.602	.712	.776	.816
FIELD 4							
Temperature	.147	.079	.057	.043	.034	.028	.024
Solar Radiation	.853	.492	.323	.241	.189	.156	.132
Initial Soil Moisture	0.0	.429	.620	.716	.776	.816	.844
FIELD 5							
Temperature	.147	.079	.057	.043	.034	.028	.076
Solar Radiation	.853	.490	.325	.242	.190	.155	.418
Initial Soil Moisture	0.0	.431	.618	.715	.776	.817	.505

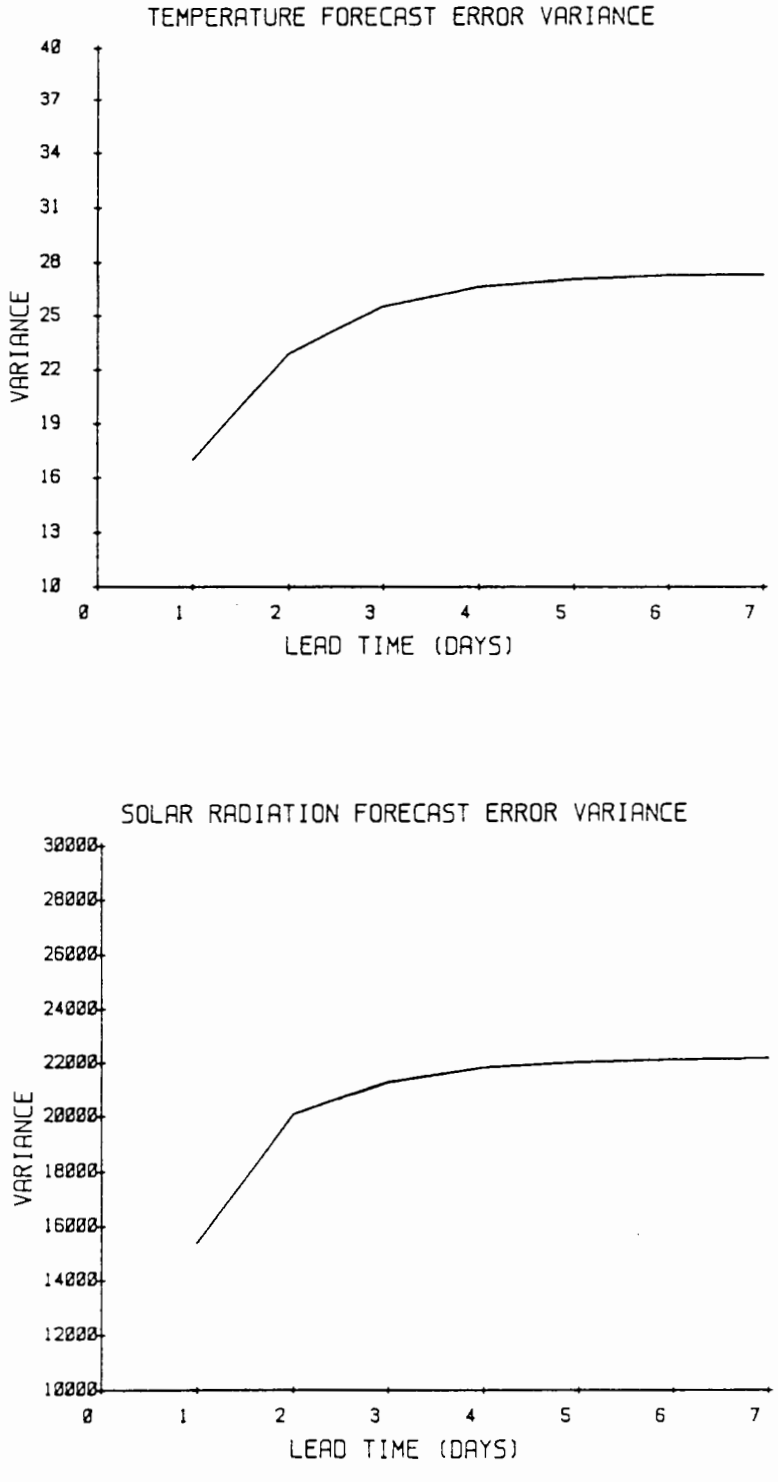

Figure 9. Temperature and solar radiation forecast error variance.

lead time increases. A one week forecast for each of the water users is provided with the system forecast.

STREAMFLOW FORECASTING

To demonstrate the streamflow forecasting model, several ARMA models are fit to the data for the main stem and tributaries in the basin. The only tributary with no record is Rock Creek. To model the flow in this stream a data set is synthesized from the records of the other tributaries. Flows from the main stem and the other tributaries for the two year period in which all of the other tributaries were gaged, are routed to the gage at Farmington using the flow routing model. The flows resulting from the routing are then subtracted from the recorded flows at the Farmington gage. This difference is used as the estimate of the flows in Rock Creek. This technique makes no allowance for losses or unaccounted for inflow that may have occurred between gages, however, this is often one of the few alternatives in such cases. This provided only a two year estimated streamflow record for Rock Creek. Presently, Scoggins Creek is fully regulated by the dam at Henry Hagg Lake, thus the flow in Scoggins Creek is deterministic as required to meet project requirements, no stochastic model is needed for this tributary.

Preliminary analysis indicates that the flows are not normally distributed as determined by the skewness test of normality (Salas et al. 1980). A logarithmic transformation performed on the data resulted in some improvement. Grouping the data into 7 day periods

helped to smooth out the statistics but provided some unrealistic correlation coefficients. Grouping the data into 14 day periods improved both the normality and the statistics probably due to the increased sample size. The 14 day grouping of data is used to fit the models. The correlation coefficients showed little or no periodicity over the May through September period, so the models are fit with constant autoregressive and moving average parameters. These statistics are shown in the Appendix. Early May tended to show slightly lower correlation coefficients that the other periods. This is probably the result of the greater inputs the system receives during this time of the year. However, since these forecasting models are typically used to model recession and not the disturbances, it is reasonable to lump May in with the rest of the season.

The main stem and each of the tributaries were fit for AR models of orders one through six and for an ARMA(1,1) model. Table X shows the residual variance of each of the models for each reach as determined from Eq. 4.16. Using the residual variance, the Akaike Information Criteria (AIC) is determined for each of the models. The AIC values are listed in Table XI. The model with the lowest AIC is selected as the best model. These models are underlined for each tributary. The parameters of the selected models are shown in Table XII and the associated residual forecast error variance is shown in Table XIII with actual error variance in Table XIV. The actual error variance is obtained by inverting the log transformed residual forecast error variance. For some of the models, the forecast variance of Table XIV peaks out at the sample variance. This was

TABLE X

RESIDUAL VARIANCE OF
STREAMFLOW MODELS

	AR(1)	AR(2)	AR(3)	AR(4)	AR(5)	AR(6)	ARMA(1,1)
Tualatin R.	.1941	.1900	.1893	.1875	.1864	.1861	.1919
Gales Cr.	.2157	.2148	.2144	.2134	.2125	.2119	.2157
McKay Cr.	.3377	.3362	.3345	.3342	.3340	.3338	.3369
Dairy Cr.	.4074	.3968	.3936	.3933	.3923	.3896	.3971
Rock Cr.	.7267	.7159	.7156	.7154	.7153	.7152	.7153

TABLE XI

AIC OF SELECTED MODELS

	AR(1)	AR(2)	AR(3)	AR(4)	AR(5)	AR(6)	ARMA(1,1)
Tualatin R.	-2757	-2787	-2795	-2809	-2817	-2817	-2774
Gales Cr.	-2579	-2584	-2586	-2591	-2596	-2599	-2577
McKay Cr.	-496	-496	-497	-495	-512	-491	-495
Dairy Cr.	-547	-562	-565	-563	-561	-565	-561
Rock Cr.	-95.9	-98.3	-96.4	-94.5	-92.5	-90.6	-98.5

TABLE XII

PARAMETERS OF SELECTED
STREAMFLOW FORECAST
MODELS

	MODEL	(1)	(2)	(3)	(4)	(5)	(6)	(1)	
Tualatin R.	AR(5)	.9682	-.1154	-.0295	.0269	.0630	-	-	.1864
Gales Cr.	AR(6)	.8726	-.0114	-.0314	.0337	.0040	.0401	-	.2119
McKay Cr.	AR(5)	.8555	-.1021	.0545	.0114	.0041	-	-	.3340
Dairy Cr.	AR(3)	.6370	.1005	.0863	-	-	-	-	.3936
Rock Cr.	AR(2)	.6887	-	-	-	-	-	.2313	.7159

TABLE XIII

RESIDUAL FORECAST ERROR VARIANCE

	Forecast Lead Time (Days)						
	1	2	3	4	5	6	7
Tualatin R.	.1864	.3611	.4871	.5670	.6208	.6692	.7149
Gales Cr.	.2119	.3670	.4862	.5667	.6268	.6731	.7164
McKay Cr.	.3340	.5784	.7109	.7919	.8483	.8897	.9189
Dairy Cr.	.3936	.5533	.6542	.7422	.8074	.8557	.8924
Rock Cr.	.7159	.8657	.9368	.9704	.9864	.9939	.9974

TABLE XIV

FORECAST ERROR
VARIANCE

	Forecast Lead Time (Days)						
	1	2	3	4	5	6	7
Tualatin R.	8.6	17.0	23.1	27.1	29.8	32.3	34.6
Gales Cr.	5.1	8.9	11.9	14.0	15.6	16.8	18.0
McKay Cr.	0.90	1.5	1.5	1.5	1.5	1.5	1.5
Dairy Cr.	13.4	15.5	15.5	15.5	15.5	15.5	15.5
Rock Cr.	0.08	0.11	0.12	0.13	0.13	0.13	0.13

imposed because the calculated inverted variance was greater than the sample variance for these lead times, so the forecast variance is set equal to the sample variance. This may result from the data not being normalized well enough with the logarithmic transformation. To improve this a more complex transformation may be required.

These models will produce forecasts that approach the mean value, which decreases as the season progresses. To demonstrate a typical forecast, the period from September 10-17, 1974 on the Tualatin River near Gaston is modeled. The forecast is shown in Figure 10 along with the actual flows that occurred. The error variance of this forecast is shown in Figure 11.

STREAMFLOW ROUTING

To demonstrate the routing model, the response of the Tualatin River to a storm during September 1974 is simulated. During this period the major tributaries were gaged and are used as known input to the river. Irrigations are assumed to be minimal during this period due to the time of year and apparent storm occurrence.

Parameter estimation was performed using bed slope and channel width data obtained from United States Geological Survey topographic quadrangle maps. The reference discharges and the celerity were estimated from published flow data for the basin (United States Geological Survey, 1974). Using Eq. 3.20 minimum and maximum reach lengths were calculated for each section of the river with relatively constant physical characteristics. Table XV shows these

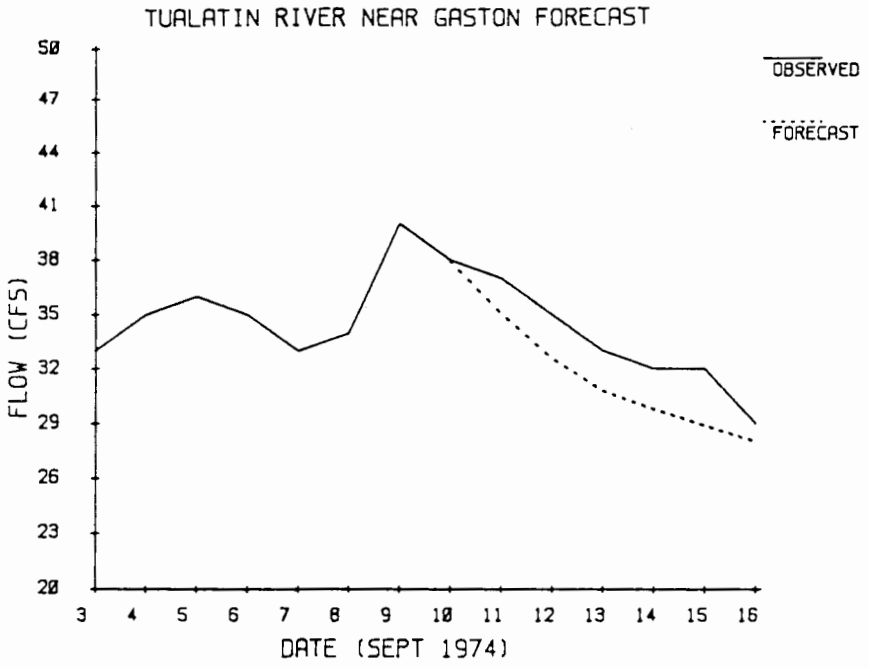

Figure 10. Tualatin River forecast.

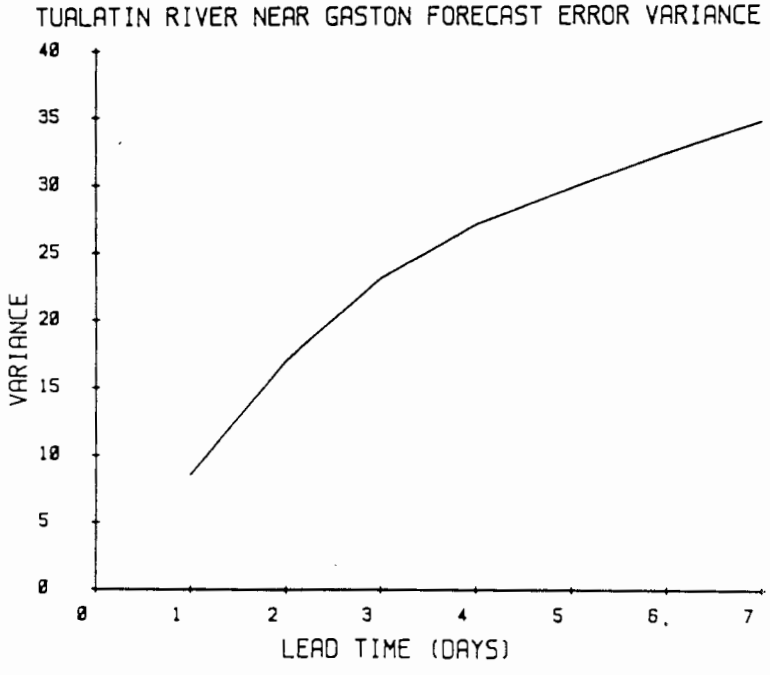

Figure 11. Tualatin River forecast error variance.

characteristics as well as the associated reach lengths. Note that the minimum reach length for the Muskingum approach is the same as the maximum reach length for the linear reservoir technique. The minimum lengths are often on the order of hundreds of feet, while the maximum is on the order of several miles, thus demonstrating the benefit of the Muskingum technique. Based on this information, reach lengths routing are set so that they correspond to the gaging stations and other landmarks in the system. The selected reach lengths and their corresponding characteristics are shown in Table XVI. The parameters K and X and the corresponding coefficients for each reach are shown in Table XVII. The elements of the A, B1, and B2 matrices are shown in Table XVIII. The results of the routing is graphed with the observed flow and are shown in Figure 12. This routing appears to be consistently low over the entire routing period. This is possibly due to a choice of reference discharges and/or other characteristics of the basin that are not realistic for the flows being routed. The flows in the system during this period were somewhat lower than the reference discharges used for parameter estimation, so this is most likely the source of error. Also, the flow estimation procedure used for Rock Creek may tend to bias the results. These results, however, appear to be sufficiently accurate to warrant the use of this model for water management purposes, as close correspondence was maintained between routed and observed flows with errors of typically only a few cubic feet per second.

TABLE XV

MUSKINGUM ROUTING REACHES
FOR THE TUALATIN RIVER
BASIN

River miles	Location	length (miles)	S (ft/ft)	B (ft)	Q (cfs)	x (miles)	x (miles)
64.8 - 60.0	End of Soggins Cr.	4.8	.00123	20	19.1	.330	15.2
65.0 - 60.0	Top of Tua. R.	5.0	.00125	20	78.4	.079	15.0
60.0 - 56.8	Confluence to Gales Cr.	3.2	.000651	20	98.8	.785	15.3
56.8 - 44.5	Gales Cr. to Dairy Cr.	12.0	.000416	20	128	1.59	15.8
44.5 - 38.2	Dairy Cr. to Rock Cr.	6.3	.000933	60	154	2.85	16.4
38.2 - 24.0	Rock Cr. to slope change	14.2	.000933	80	158	1.43	15.7
24.0 - 9.5	slope change to Fanno Cr.	14.5	.000949	110	158	1.57	15.7
9.5 - 5.5	Fanno Cr. to Oswego Canal	4.0	.000214	120	201	.810	15.4
5.5 - 1.7	Oswego Canal to slope change	3.8	.00399	120	147	.434	15.2
1.7 - 0	Slope change to Willamette R.	1.7	.00405	120	147	.0284	15.0

TABLE XVI

PHYSICAL PROPERTIES OF SELECTED REACHES

REACH	LENGTH (miles)	S (ft/ft)	B (ft)	Q (cfs)
1	4.8	0.00123	20	19.1
2	3.9	0.00125	20	78.4
3	1.2	0.000651	20	98.8
4	3.4	0.000651	20	98.8
5	3.9	0.000416	20	128.0
6	7.1	0.000416	20	128.0
7	5.9	0.0000933	60	154.0
8	5.2	0.0000933	80	158.0

TABLE XVII

ROUTING PARAMETERS AND COEFFICIENTS

REACH	K (days)	X	C1	C2	C3
1	0.1600	0.4916	0.9953	0.7248	-0.7202
2	0.1300	0.4584	0.9810	0.7721	-0.7531
3	0.0400	0.1728	0.9509	0.9250	-0.8759
4	0.1133	0.3845	0.9541	0.8011	-0.7552
5	0.1300	0.2959	0.9103	0.7802	-0.6905
6	0.2367	0.3879	0.9177	0.6330	-0.5507
7	0.1967	0.2587	0.8530	0.6954	-0.5484
8	0.1733	0.2893	0.8828	0.7219	-0.6047

TABLE XVIII

A, B1, AND B2
MATRICIES

$$A = \begin{bmatrix} -.7202 & 0 & 0 & 0 & 0 & 0 & 0 & 0 \\ 0 & -.7531 & 0 & 0 & 0 & 0 & 0 & 0 \\ .2847 & .2543 & -.8759 & 0 & 0 & 0 & 0 & 0 \\ .2281 & .2037 & .2497 & -.7552 & 0 & 0 & 0 & 0 \\ .1780 & .1589 & .1948 & .3211 & -.6905 & 0 & 0 & 0 \\ .1127 & .1006 & .1233 & .2033 & .4806 & -.5507 & 0 & 0 \\ .0783 & .0700 & .0858 & .1413 & .3342 & .4700 & -.5484 & 0 \\ .0565 & .0505 & .0619 & .1020 & .2413 & .3393 & .4869 & -.6047 \end{bmatrix}$$

$$B1 = \begin{bmatrix} .9953 & 0 & 0 & 0 & 0 & 0 & 0 & 0 \\ 0 & .9810 & 0 & 0 & 0 & 0 & 0 & 0 \\ .9207 & .9074 & .9509 & 0 & 0 & 0 & 0 & 0 \\ .7375 & .7269 & .7618 & .9541 & 0 & 0 & 0 & 0 \\ .5754 & .5672 & .5943 & .7444 & .9103 & 0 & 0 & 0 \\ .3642 & .3590 & .3762 & .4712 & .5762 & .9177 & 0 & 0 \\ .2533 & .2497 & .2616 & .3277 & .4007 & .6382 & .8530 & 0 \\ .1829 & .1802 & .1889 & .2365 & .2893 & .4607 & .6158 & .8828 \end{bmatrix}$$

$$B2 = \begin{bmatrix} .7248 & 0 & 0 & 0 & 0 & 0 & 0 & 0 \\ 0 & .7721 & 0 & 0 & 0 & 0 & 0 & 0 \\ .6704 & .7142 & .9250 & 0 & 0 & 0 & 0 & 0 \\ .5371 & .5721 & .7410 & .8011 & 0 & 0 & 0 & 0 \\ .4190 & .4464 & .5781 & .6250 & .7802 & 0 & 0 & 0 \\ .2653 & .2826 & .3660 & .3956 & .4939 & .6330 & 0 & 0 \\ .1845 & .1965 & .2545 & .2751 & .3434 & .4402 & .6954 & 0 \\ .1332 & .1418 & .1837 & .1986 & .2479 & .3178 & .5020 & .7219 \end{bmatrix}$$

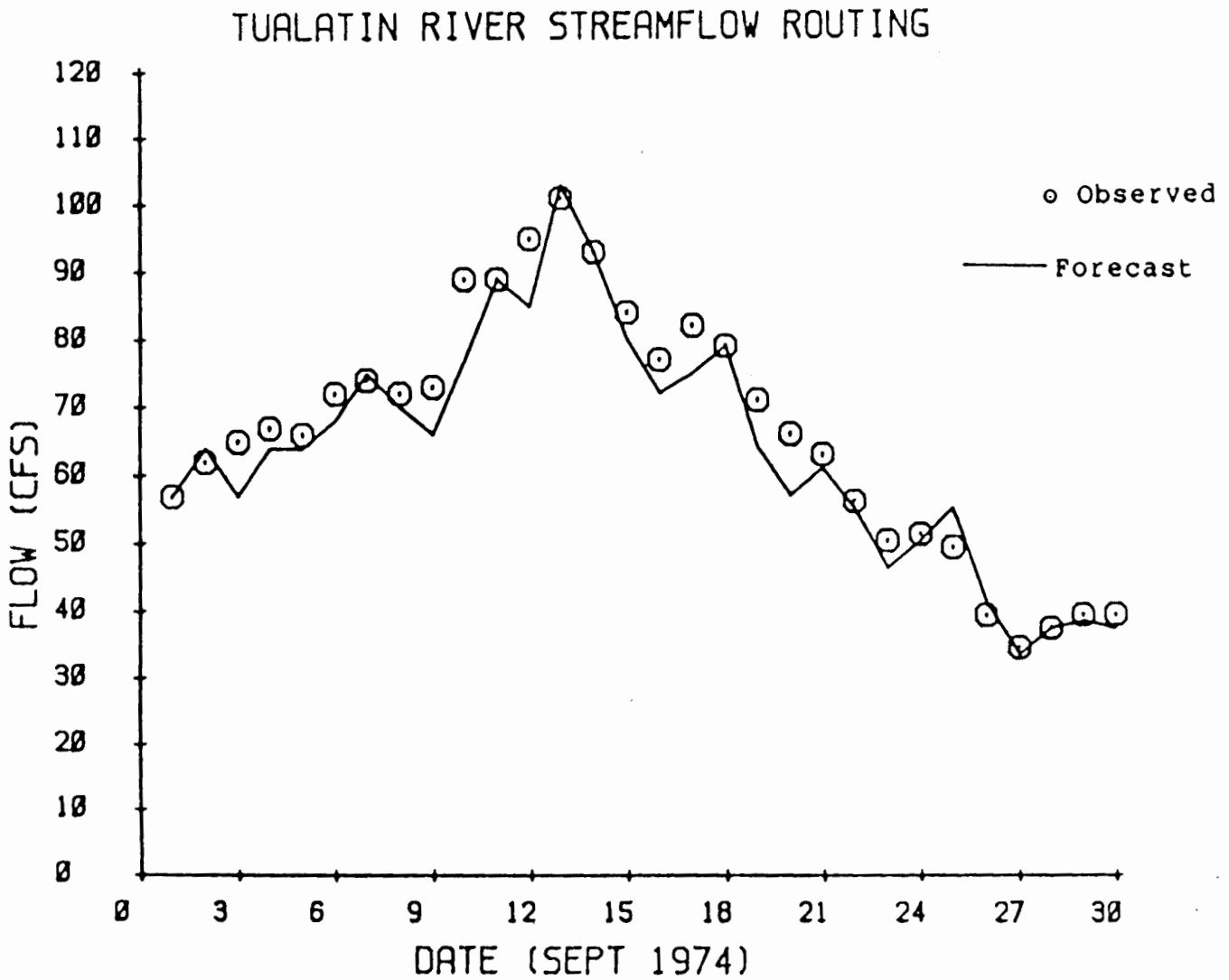

Figure 12. Comparison of modeled and observed discharge of the Tualatin River.

SYSTEM FORECAST

To demonstrate the interaction of all the models, a forecast for the seven day period from July 25 through July 31, 1974 is performed. This period is chosen because it provides most of the data needed to compare the forecasts to observed values, particularly on the major tributary streams. No solar radiation data are available for this time period, so a set of synthesized values is used for comparison. These data are synthesized using the MVAR generation model with the temperature equal to the observed temperature. The result is a solar radiation data set with the same multivariate relationships that occur in the historic record. Soil moisture data are also not available for this period and 'reasonable values' are chosen to provide the initial conditions required by the model so that they adequately demonstrate model response to different soil/crop conditions. The final result of the entire system forecast is the steamflow in the Tualatin River at the Farmington gage. During this time period, however, the irrigation diversions were not known and cannot be used as input. Furthermore, the dam on Scoggins Creek was not yet in place and actual or forecast flows might not be able to meet irrigation demands that one might encounter. So, to realistically simulate the system, some assumptions and modifications have to be made. These are as follows. To accommodate irrigation demands on Scoggins Creek, the flows in Scoggins Creek will be set at 25 cfs as though a dam was controlling the releases. Synthesized values of solar radiation are to be used as described above and initial conditions of soil moisture are chosen and

indicated in Table VIII. The 'observed' soil moisture is taken as the results of the soil moisture model with the observed values of temperature and synthesized values of solar radiation as input. The 'observed' flows in the Tualatin River at the Farmington gage are taken as the routed observed inflows and diversions from the system. These modifications and assumptions imply a perfect soil moisture and routing model, which is clearly not the case. However, comparison of forecasts with the observations provides insight to the forecast errors.

July 24 had no precipitation which results in a forecast of zero precipitation over the seven day period. The temperature and solar radiation forecasts and observed values are shown in Figure 13. The initial temperature is very close to the mean value for this period and so the forecast showed little variation. The solar radiation forecast also showed little variation from its initial condition. The forecast error variance of these forecasts were presented earlier in Figure 9. From these forecasts water requirement of the irrigated lands is calculated. When the water requirement is forecast to be below the critical available water, an irrigation is assumed during that day to bring the available water up to field capacity. The forecasts of available water are shown in Table XIX with the observed soil moisture in Table XX. The forecast error variance of these forecasts are shown in Table XXI. From these forecasts, it can be seen that two fields need to be irrigated. The forecast soil moisture for these fields are shown in Figures 14 and 15. The flows needed to meet these requirements, and the variance of these flows are in Table

TABLE XIX

AVAILABLE WATER FORECAST
JULY 25 - 31, 1974

	DATE JULY, 1974						
Field Number	25	26	27	28	29	30	31
1	.139	.129	.117	.110	.102	.094	.087
2	.157	.146	.135	.126	.112	.103	.095
3	.123	.117* (.200)	.189	.179	.170	.161	.153
4	.207	.196	.185	.175	.165	.156	.147
5	.104	.098	.093	.088	.083	.078* (.180)	.170

TABLE XX

OBSERVED AVAILABLE WATER
JULY 25 - 31, 1974

	DATE JULY, 1974						
Field Number	25	26	27	28	29	30	31
1	.142	.131	.119	.109	.097	.083	.077
2	.167	.154	.140	.128	.114	.097	.090
3	.125	.118* (.200)	.187	.173	.159	.141	.133
4	.211	.199	.185	.173	.159	.141	.133
5	.106	.100	.093	.087	.080	.071* (.180)	.170

For both tables the numbers with an '*' indicate that an irrigation is required. The numbers in parantheses show the available water content following the irrigation.

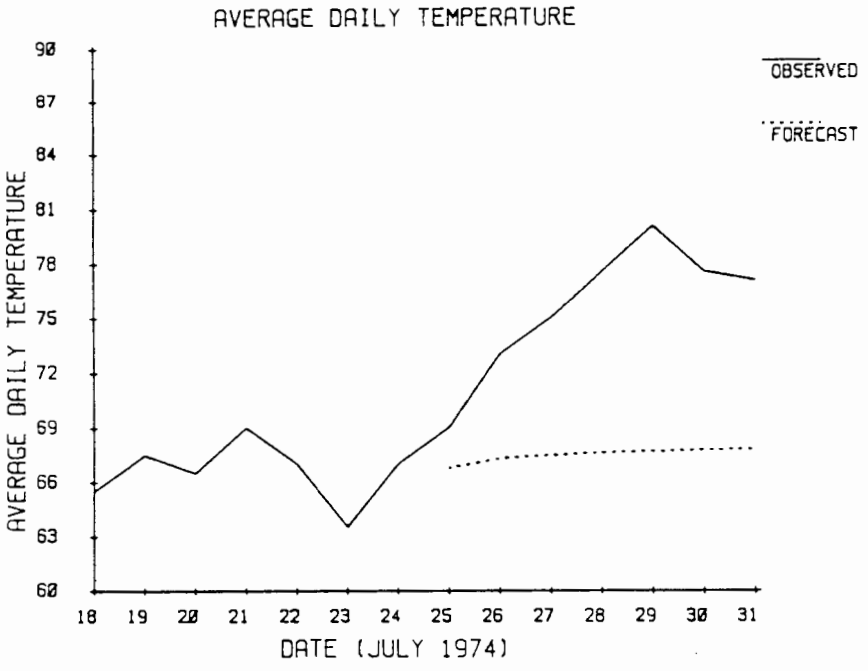

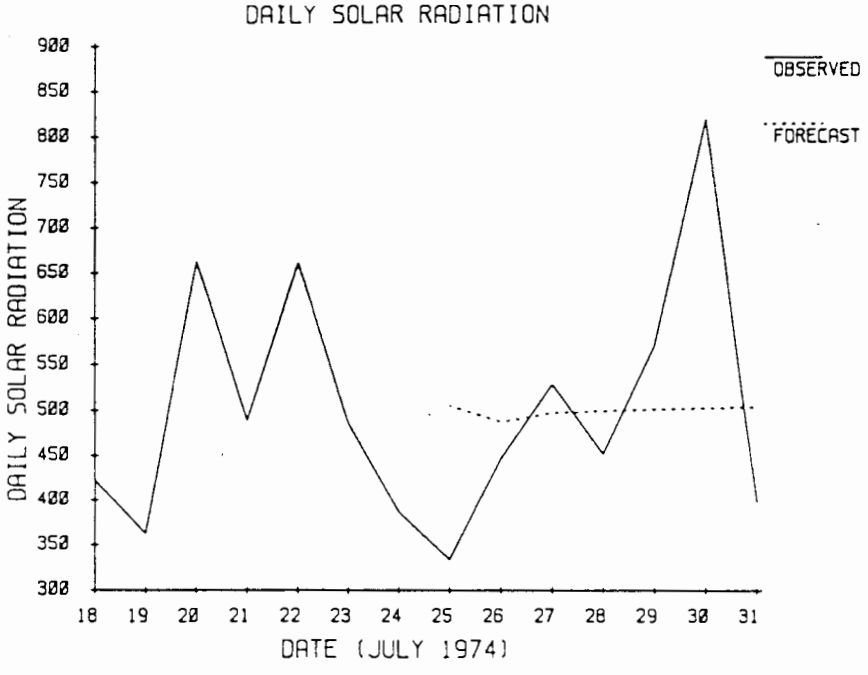

Figure 13. 7 day temperature and solar radiation forecast.

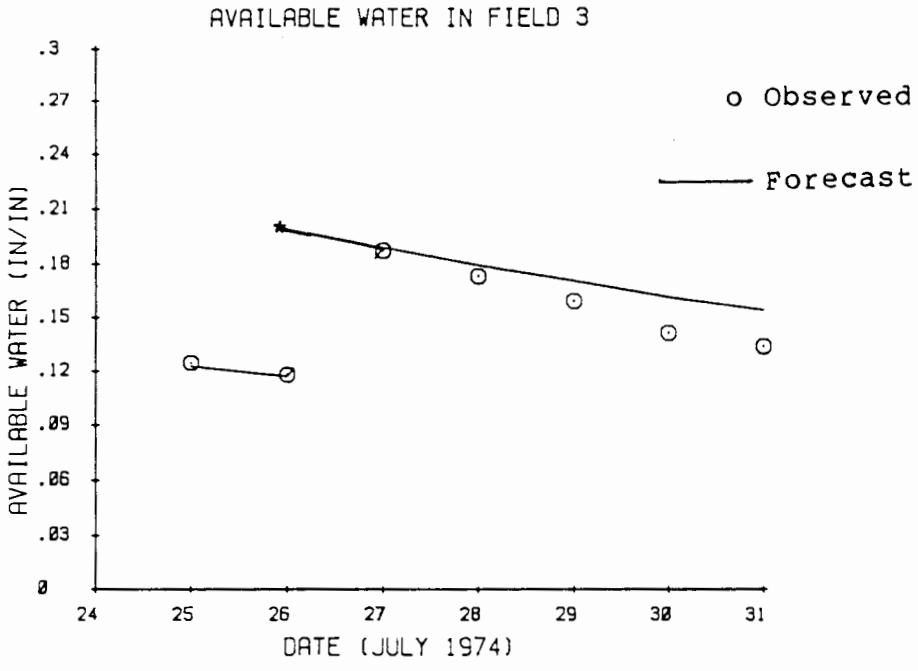

Figure 14. Available water forecast for field 3.

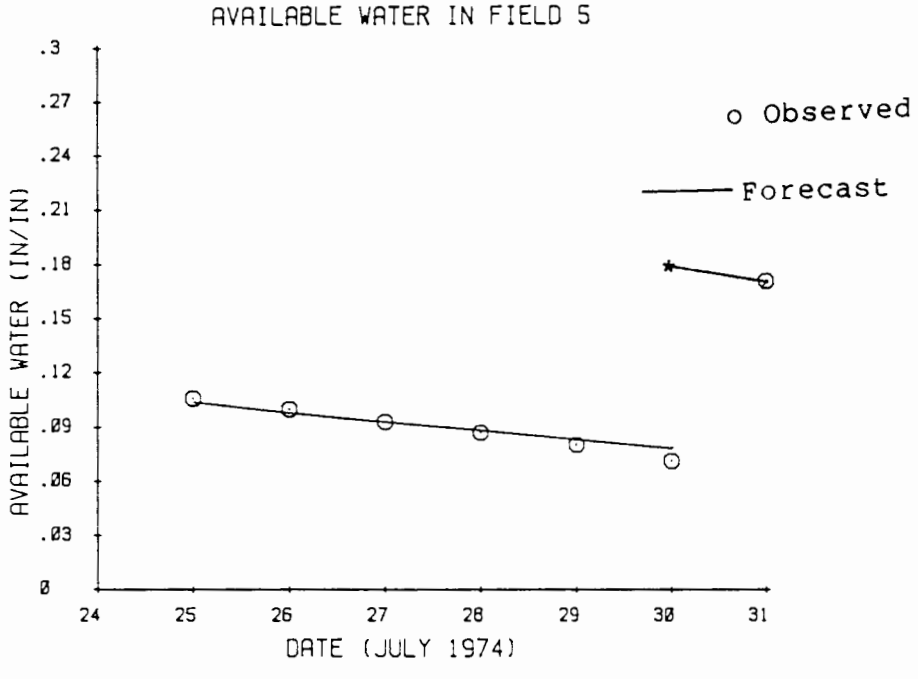

Figure 15. Available water forecast for field 5.

A * indicates the soil moisture following an irrigation.

XXII. For use in routing computations these demands are treated as output from the top of the appropriate reach. Streamflow forecasts and observed values are shown in Tables XXIII and XXIV and are presented graphically in Figures 16 through 20. The irrigation demands and the streamflow forecasts are used as inputs to the routing model. The results of this routing are shown in Figure 21.

The errors of the forecasts are propagated using equation 4.26. Table XXV shows the error covariance matrices for lead times of one and two days. The matrices for lead time three through seven days are presented in the Appendix. The diagonal terms of these matrices are the forecast error variance. They tend to grow rapidly at first and then level off as the lead time increases. Figures 22 and 23 shows these variances for reaches 2 and 5 respectively.

TABLE XXI

FORECAST ERROR VARIANCE
OF AVAILABLE WATER
JULY 25 - 31, 1974
(* 10^5)

DATE JULY, 1974

Field Number	25	26	27	28	29	30	31
1	0.71	1.42	1.94	2.31	2.55	3.04	3.01
2	0.91	1.82	2.52	3.01	3.27	3.85	3.79
3	0.26	0.55	1.37	2.05	2.59	3.23	3.51
4	0.90	1.87	2.70	3.35	3.84	4.58	4.76
5	0.23	0.47	0.68	0.85	0.97	1.15	1.94

TABLE XXII

IRRIGATION DIVERSIONS
JULY 25 - 31, 1974
(CFS)

DATE JULY, 1974

	25	26	27	28	29	30	31
REACH 1 Field 5							
Forecast	0	0	0	0	0	13.9 (0.14)	0
Observed	0	0	0	0	0	14.8	0
REACH 8 Field 3							
Forecast	0	21.9 (0.26)	0	0	0	0	0
Observed	0	21.7	0	0	0	0	0

None of the other reaches have forecast or actual diversions during this time period. Forecast error variances are in parentheses.

TABLE XXIII

STREAMFLOW FORECAST
JULY 25 - 31, 1974
(CFS)

	Date, July 1974						
	25	26	27	28	29	30	31
Tualatin R.	20.1	19.2	18.2	17.6	17.4	17.3	17.2
Gales Cr.	14.7	14.2	13.5	13.0	12.6	12.4	12.3
McKay Cr.	4.5	3.5	3.0	2.8	2.6	2.4	2.3
Dairy Cr.	13.5	12.4	12.0	11.5	11.1	10.7	10.4
Rock Cr.	0.67	0.57	0.29	0.18	0.15	0.12	0.10
Routed Forecasts to Farmington Gage	82.4	49.5	61.4	77.8	51.7	46.8	33.3

TABLE XXIV

OBSERVED STREAMFLOW
JULY 25 - 31, 1974
(CFS)

	Date, July 1974						
	25	26	27	28	29	30	31
Scoggins Cr.	25.0	25.0	25.0	25.0	25.0	25.0	25.0
Tualatin R.	19.0	17.0	20.0	20.0	19.0	18.0	17.0
Gales Cr.	14.0	13.0	13.0	10.0	9.6	9.0	7.8
McKay Cr.	3.8	3.1	3.2	1.4	1.8	1.6	0.7
Dairy Cr.	17.0	15.0	10.0	11.0	13.0	10.0	9.3
Rock Cr.	10.0	0.0	0.0	0.0	0.0	0.0	0.0
Routed Observations to Farmington Gage	83.1	52.8	64.5	77.0	46.5	35.7	28.3

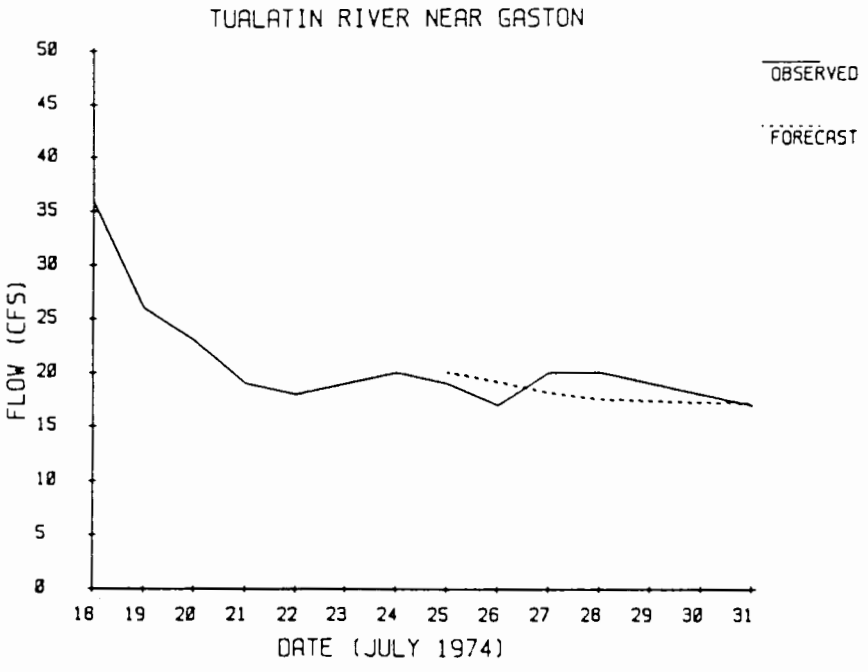

Figure 16. Forecast and observed flow in the Tualatin River near Gaston.

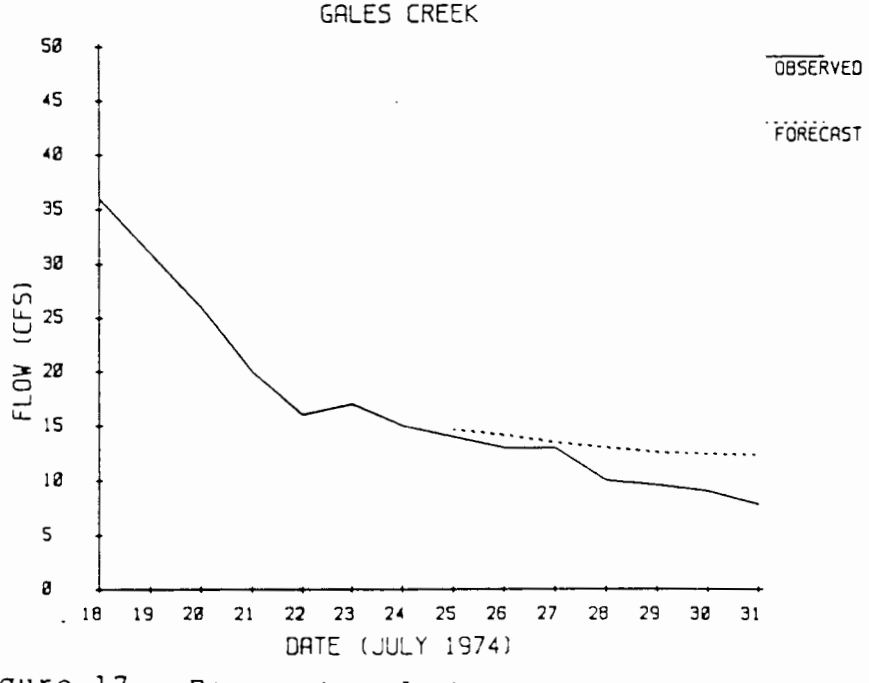

Figure 17. Forecast and observed flows in Gales Creek.

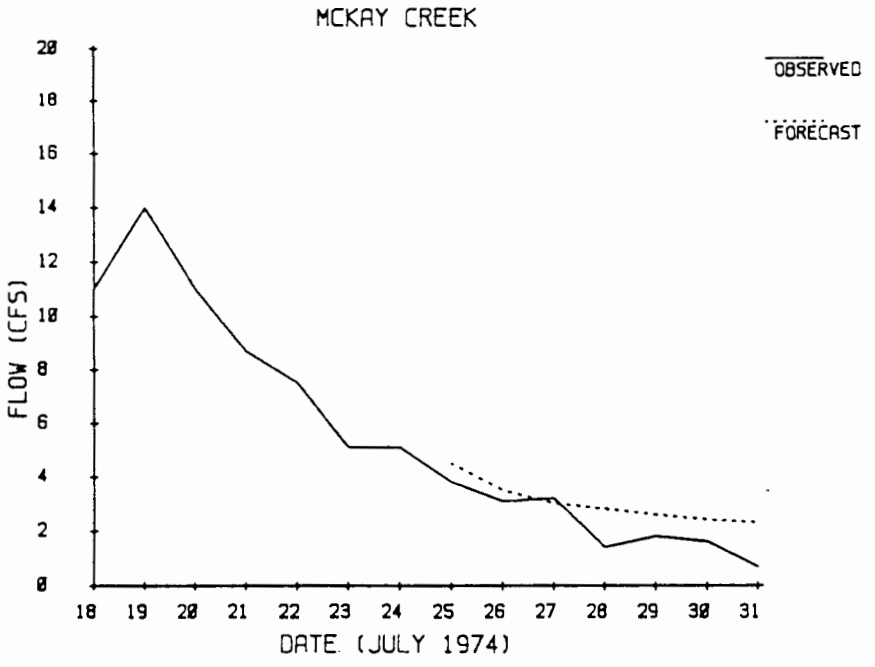

Figure 18. Forecast and observed flows in McKay Creek.

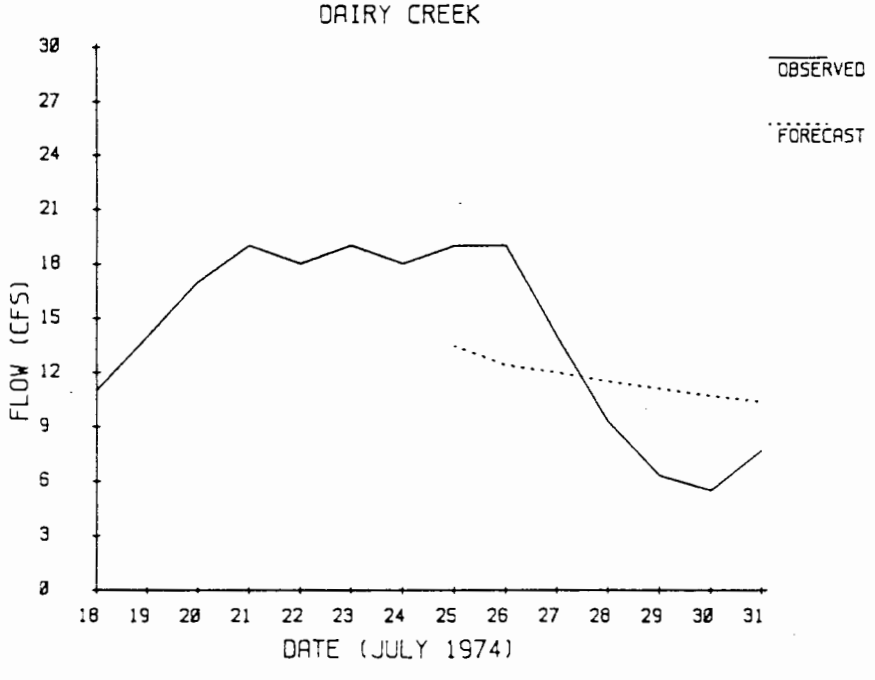

Figure 19. Forecast and observed flows in Dairy Creek.

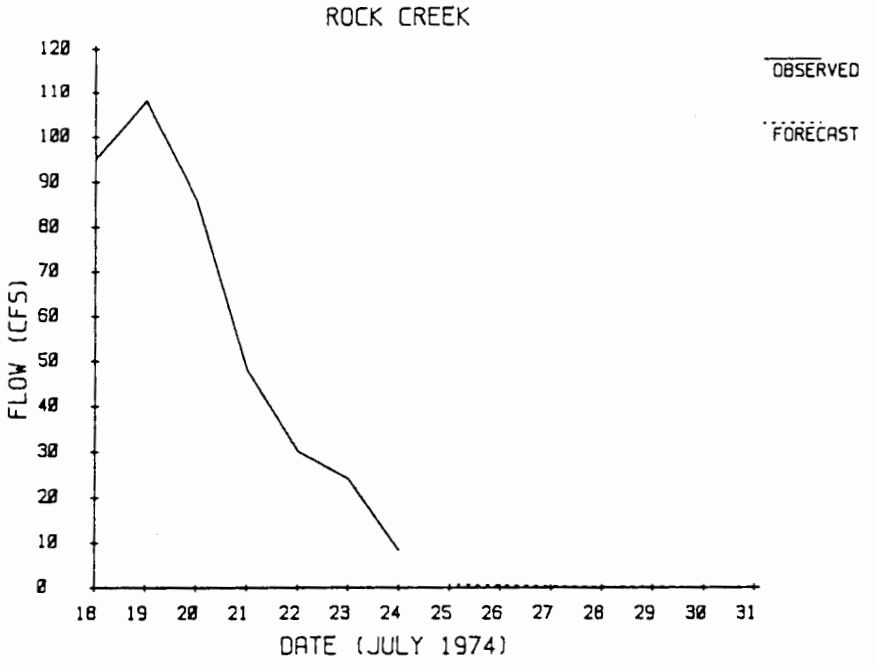

Figure 20. Forecast and observed flows in Rock Creek.

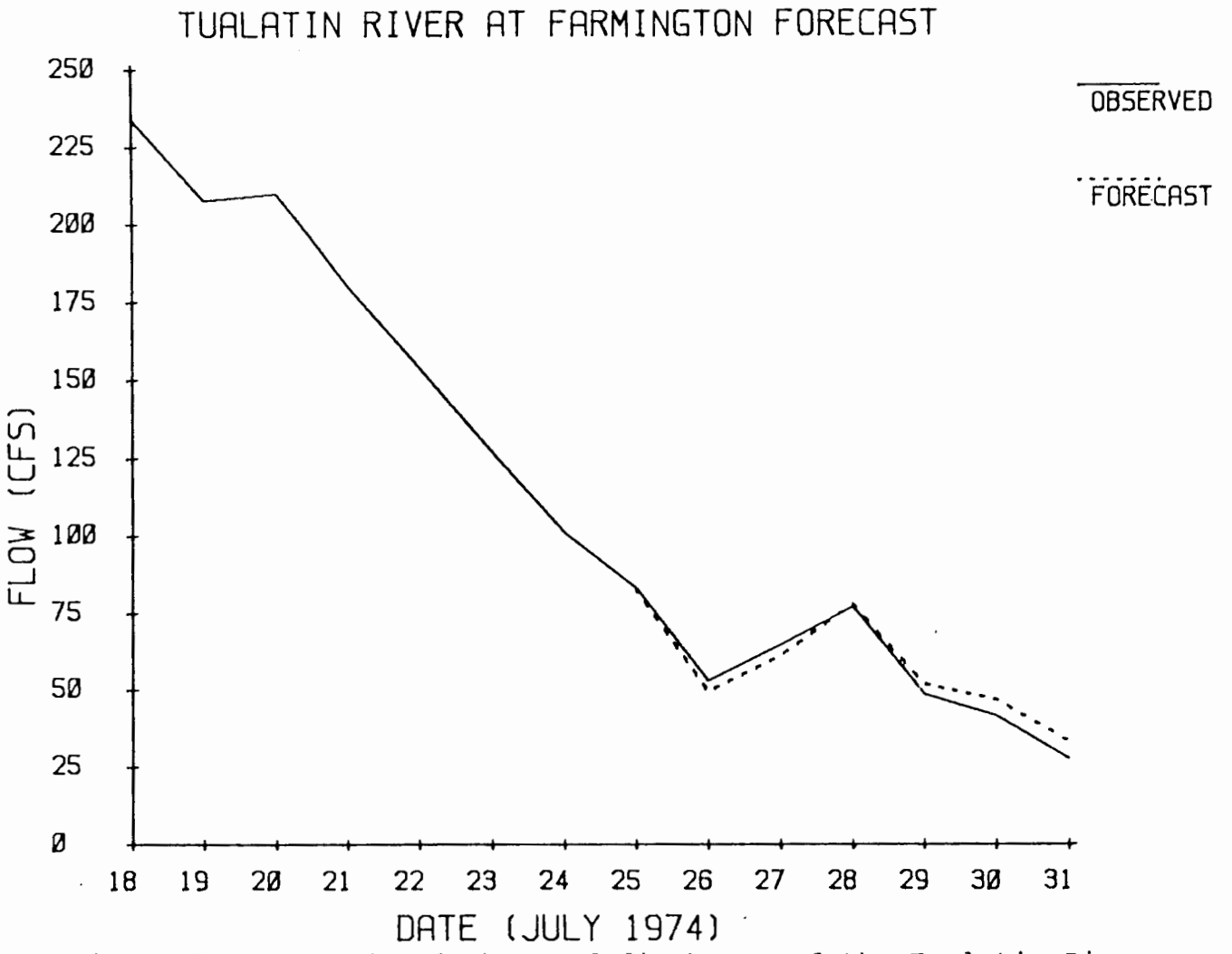

Figure 21. Routed and observed discharge of the Tualatin River near Farmington, Oregon.

TABLE XXV

FORECAST ERROR COVARIANCE MATRICES
FOR LEAD TIMES OF 1 AND 2 DAYS

1 Day Lead Time

0.000	0.000	0.000	0.000	0.000	0.000	0.000	0.000
0.000	8.276	7.655	6.133	4.785	3.029	2.107	1.520
0.000	7.655	7.081	5.672	4.426	2.802	1.949	1.406
0.000	6.133	5.672	9.187	7.168	4.537	3.156	2.277
0.000	4.785	4.426	7.168	17.442	11.041	7.678	5.543
0.000	3.029	2.802	4.537	11.041	6.988	4.860	3.508
0.000	2.107	1.949	3.156	7.678	4.860	3.380	2.440
0.000	1.520	1.406	2.277	5.543	3.508	2.440	1.824

2 Day Lead Time

0.000	0.000	0.000	0.000	0.000	0.000	0.000	0.000
0.000	26.181	23.340	16.700	11.315	6.192	2.479	1.080
0.000	23.340	20.942	15.302	10.673	6.040	2.852	1.535
0.000	16.700	15.302	17.847	12.338	6.912	3.117	1.594
0.000	11.315	10.673	12.338	38.098	21.931	11.133	6.441
0.000	6.192	6.040	6.912	21.931	13.762	9.344	6.658
0.000	2.479	2.852	3.117	11.133	9.344	10.826	9.492
0.000	1.080	1.535	1.594	6.41	6.658	9.492	11.185

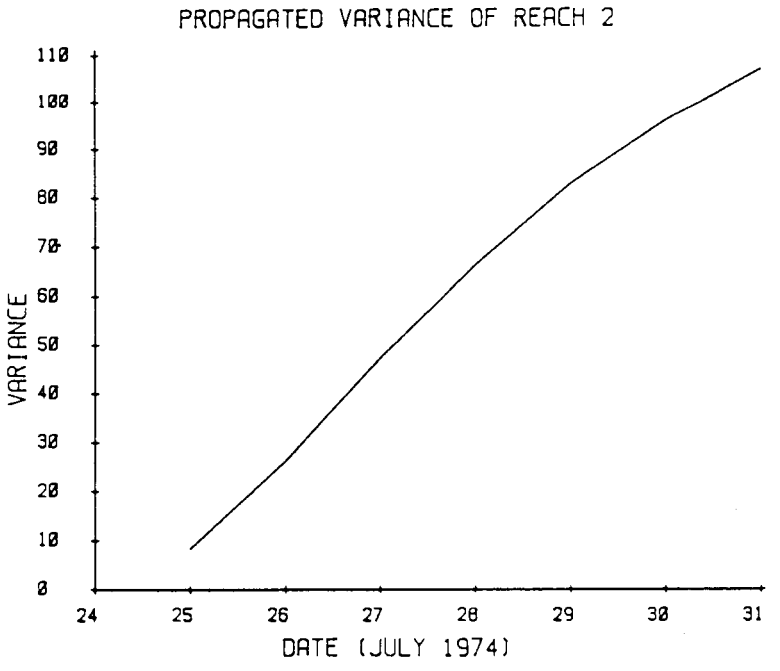

Figure 22. Propagated forecast error variance for reach 2.

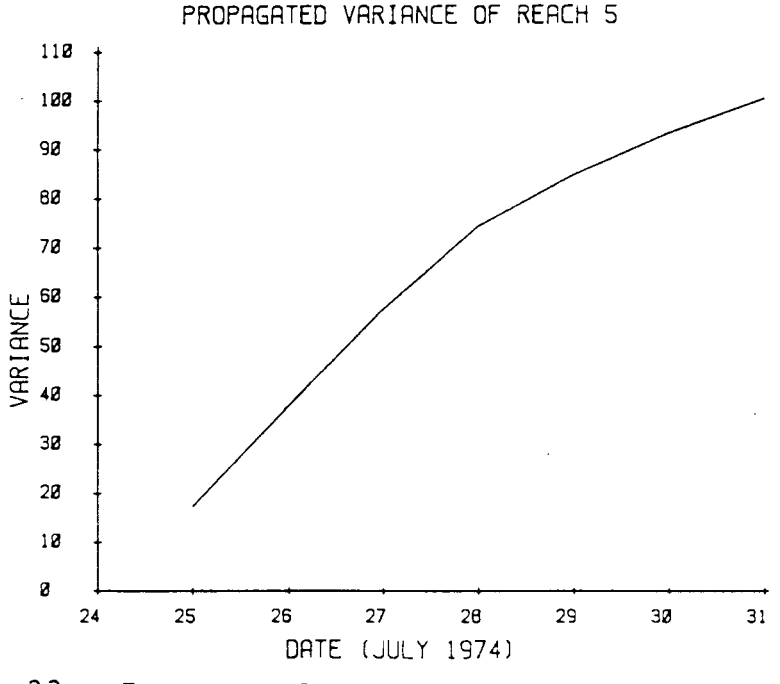

Figure 23. Propagated forecast error variance for reach 5.

EVALUATION

This chapter demonstrates each of the forecast models and used their output as the inputs to the soil moisture and routing models to obtain a routed streamflow forecast. The temperature and solar radiation models did not provide forecasts that maintain close correspondence to the observed values. However, the soil moisture model is relatively insensitive to these forecasts, resulting in forecasts of soil moisture that are very close to the observed soil moisture. The streamflow forecast models appear to perform reasonably well for most of the tributaries. Using the results of the forecast models as input to the routing model produced streamflow at Farmington that is very close to the routing of the observed inputs.

The simplifications and modifications required to fit and use the models and compare the output to the observations must be considered. Great effort was taken to ensure that these examples be as realistic as possible given the data that were available. Simplification was kept to a minimum and modifications were made only when data was insufficient to fit models. Overall, the results of these examples tend to show that the models presented are capable of providing forecasts whose results are sufficiently accurate for use as a guide in water management.

CHAPTER VI

SUMMARY AND CONCLUSIONS

This paper presents several models intended for use in water management with methods for evaluating forecast model errors. The forecast models are for preciptation quantity, temperature, solar radiation and streamflow. Precipitation, temperature, and solar radiation forecasts are used as the inputs to a soil moisture model which provides irrigation diversion requirements. The forecast streamflows and irrigation requirements serve as input to a routing model that provides streamflow forecasts throughout a river basin. These forecasts are used to indicate whether diversions can be met with the existing operating policy or conditions, or if a new policy must be implemented. The precipitation forecast model uses simple Markov transition probabilities to determine precipitation quantity given the precipitation quantity on the previous day. The model selected for temperature and solar radiation is a multivariate autoregressive model using different parameters based on precipitation. The streamflow forecast models are of the autoregressive-moving average type. To route forecast inflows and diversions a state space approach to the Muskingum-Cunge routing technique is applied. The errors of the forecast models and the propagation of errors through the models are investigated.

CONCLUSIONS

Each of the component models seem to provide reasonable forecasting capabilities for use with soil moisture modeling and streamflow routing. The precipitation model is simplistic, and not capable of forecasting rain when no rain has occurred on the previous day. However, for use in an irrigation management model, where the objective is to ensure that enough water is available to meet crop demends, this model provides conservative estimates, which are generally desireable. Unfortunately, this could also lead to wasted water if rain did occur when none was forecast. This model is well suited to areas where there are typically several days of dry weather in a row. In the system forecast the precipitaion model forecast zero rain for the seven day period.

The temperature and solar radiation model did not perform well in the system forecast. The forecast error variance rapidly approached the sample variance, indicating the model to be of relatively little value. This is probably due to the non-continuous set of solar radiation data from which the parameters were estimated. A more complete set of data would be likely to improve model performance substantially.

The soil moisture forecasts, driven by the temperature and solar radiation, showed little sensitivity to these forecasts. This resulted in soil moisture forecasts that were very close to the soil moisture under the simulated conditions.

The streamflow forecasting models indicate that reasonably good forecasts can be obtained when the stream is in recession. For

periods in which the streamflow is fluctuating, ARMA forecast models do not perform well. For the streams modeled in this study, it is apparent that use of long flow records for parameter estimation produced forecasting models with lower error variance than those estimated from short data sets. This further demonstrates the need for complete, long data sets to obtain good stochastic models.

The Muskingum-Cunge routing technique is slightly more complex in form than the linear reservoir technique but allows for much longer reach lengths while still maintaining physical correspondence with the system being modeled. This provides accurate routing with far fewer reaches resulting in a considerable savings in computation time. The general solution to the state space formulation of the Muskingum routing method is far too cumbersome to be useful for practical application. However, the state equation may be easily used to provide one step ahead forecasts to as many time steps into the future as required by using the results from one time step as the initial conditions for the next. This matrix approach may also have considerable utility when used with vector processers that are being developed for computers.

The results of the system forecast indicate that the proposed forecast and routing models could be adequate for use in water management for simple systems with only a few water users. Further testing is required, under a variety of conditions, to determine when and where the models can be successfully used. Further interpretation of the forecast error covariance matrices may also be of some use.

Implementation of these models requires periodic updating, possibly every one or two days particularly when conditions change rapidly, such as the occurrence of a rainstorm. In a small basin, where the river travel time is only a few days, such updating could provide enough information to make operational changes in time to prevent short term water shortages in the river or prevent water from being wasted.

A major drawback to these forecast models is the amount of data required to accurately estimate the parameters. Temperature records are generally readily available but good records of solar radiation are not common. Each of the major tributaries must have at least a few years of data as well. This requires that the need for future forecasting capabilities be realized with enough time to install gaging and measurement equipment so that a good data base is established by the time the models are required. Another drawback may be encountered by the computer resources that are required to run a comprehensive water management model incorporating the proposed forecast and routing models The models presented are relatively simple, but when combined with a system that keeps track of the pertinent water user information, the system can become quite complex requiring substantial computing capabilities. However, computers are rapidly becoming more powerful and less expensive, so it is not unreasonable to expect that the necessary computing capabilities are likely to be available to water managing agencies.

With all of this in mind, these forecasting models and the streamflow routing model, when combined with an adequate data base and a comprehensive water management model, are capable of being a powerful tool to aid water managers in the day to day operational strategies required for local water management.

BIBLIOGRAPHY

Allen, Roderick Lee, 1985. "The applicability of Microcomputers to Local Water Management." A Thesis submitted in partial fulfillment for the degree of Master of Science in Engineering: Civil. Portland State University, 1985.

Box, G. E. P. and G. M. Jenkins, Time Series Analysis: Forecasting and Control, Holden-Day, 1970.

Bruhn, J. A. and W. E. Fry, and G. W. Fick, 1980. "Simulation of Daily Weather Using Theoretical Probability Distributions." Journal of Applied Meteorology, 19, No. 9, pp. 1029-1036.

Cunge, J. A., 1969. "On the Subject of a Flood Propagation Computation Method (Muskingum Method)." Journal of Hydraulic Research, 7, No. 2, pp. 205 - 230.

Gelb, Arthur, (editor), Applied Optimal Estimation. The MIT Press, 1974

Haan, C. T., H. P. Johnson, and D. L. Brakensiek, editors. Hydrologic Modeling of Small Watersheds. American Society of Agricultural Engineers, 1982.

Khanal N. N. and R. L. Hamrick, "A Stochastic Model For Daily Rainfall Data Synthesis." Proceedings Symposium on Statistical Hydrology, Arzona University, Tuscon, August 31 - September 2, 1973. Miscellaneous Publication No. 1275, pp. 190 - 210, June 1974.

Koch, R. W. and R. L. Allen, 1985. "A Simple, Physically Based Model of Soil Moisture." Submitted to the Journal of Irrigation and Drainage Engineering, ASCE.

Koussis, Antonis, 1983. Discussion of "Accuracy Criterion in Diffusion Routing." Journal of the Hydraulics Division, 7, No. 5, pp. 803 - 807.

Loague, Keith M. and R. Allen Freeze, 1985, "A Comparison of Rainfall-Runoff Modeling Techniques on Small Upland Catchments. Water Resources Research, 21, No. 2 pp. 229 - 248.

Miller, Robert B., William Bell, Osvaldo Ferreiro, and Richard Yng-Yuh Wang, 1981. "Modeling Daily River Flows With Precipitation Input." Water Resources Research, 17, No. 1, pp 209 - 215.

O'Connell, Patrick E., 1979 "Shot Noise Models in Synthetic Hydrology." in Mathematical Models for Surface Water Hydrology. T.A. Ciriani, U. Maione, and J. R. Wallis, editors. John Wiley and Sons, New York, 1979.

Ponce, Victor Miquel and Fred D. Theurer, 1982. "Accuracy Criteria in Diffusion Routing." Journal of the Hydraulics Division, ASCE, 108, No. HY6, pp. 747 - 757.

Ponce, V. M., R. M. Li, and D. B. Simons, 1978. "Applicability of Kinematic and Diffusive Models." Journal of the Hydraulics Division, ASCE, 104, pp. 353 - 360.

Ponce, V. M. and V. Yevjevich, 1978. "Muskingum-Cunge Method With Variable Parameters." Journal of the Hydraulics Division, ASCE, 104, pp. 1663 - 1667.

Richardson, C. W., 1981. "Stochastic Simulation of Daily Precipitation, Temperature and Solar Radiation." Water Resources Research, 18, No. 1, pp. 182 - 190.

Salas, Jose D., Duane C. Boes, and Ricardo A. Smith, 1982. Estimation of ARMA Models With Seasonal Parameters." Water Resources Research, 18, No. 4, pp 1006 - 1010.

Salas, J. D. and J. T. B. Obeysekera, 1982. "ARMA Model Identification in Hydrologic Time Series." Water Resources Research, 18, No. 4, pp. 1011 - 1021.

Salas, J. D., J. W. Delleur, V. Yevjevich, and W. L. Lane. Applied Modeling of Hydrologic Time Series. Water Resources Publications, 1980.

Sargent, D. M., 1979. "A Simplified Model For The Generation of Daily Streamflows." Hydrologic Sciences Bulletin, 24, No. 4, pp. 509 - 527.

Saxton, K. E. and J. L. McGuinness, 1982. "Evapotranspiration" in Hydrologic Modeling of Small Watersheds. Haan, C. T., H. P. Johnson, and D. L. Brakersiek, Ed., St. Joseph, MI: American Society of Agricultural Engineers.

Todorovic, P. and D. Woolhiser, Stocastic Model of Daily Rainfall." Proceedings Symposium on Statistical Hydrology, Arizona University, Tuscon, August 31 - September 2, 1973. Miscellaneous Publication No. 1275, pp. 232 -245, June 1974.

Viessman, Warren Jr., John W. Knapp, Gary L. Lewis, Terence E. Harbaugh. Introduction to Hydrology. Harper and Row, Publishers Inc. 1977.

Weinmann, Erwin P. and Eric Laurenson, 1979. "Approximate Flood Routing Methods: A Review." Journal of the Hydraulics Division, ASCE, 105, No. HY12, pp. 1521 - 1536.

Yakowitz, Sidney J.,1979 "A Nonparametric Model for Daily River Flow." Water Resources Research, 15, No. 5, pp 1035 - 1043.

Yazicigil, Hasan, A. Ramachandra Rao, and G. H. Toebes, 1982. Investigation of Daily Flow Forecasting Models." Journal of Water Resources Planning and Management Division, ASCE, 108, No. WR1, March, 1982.

APPENDIX

TABLE XXVI

PRECIPITATION TRANSITION PROBABILITIES
FOREST GROVE, OREGON

May 1 - May 12

.771	.092	.040	.032	.016	.012	.036
.453	.156	.141	.078	.031	.063	.078
.345	.241	.103	.000	.034	.103	.172
.571	.214	.143	.000	.071	.000	.000
.308	.385	.000	.000	.154	.077	.077
.231	.154	.231	.077	.077	.154	.077
.250	.375	.042	.000	.083	.000	.250

May 13 - May 26

.805	.103	.019	.031	.015	.011	.015
.534	.155	.138	.000	.017	.052	.103
.423	.346	.077	.038	.038	.000	.077
.214	.143	.214	.143	.000	.000	.286
.286	.143	.286	.000	.000	.143	.143
.429	.143	.143	.000	.000	.000	.286
.121	.303	.091	.152	.030	.000	.303

May 27 - June 9

.793	.088	.034	.034	.014	.000	.037
.542	.250	.021	.042	.021	.021	.104
.471	.176	.118	.118	.000	.000	.118
.412	.176	.059	.176	.059	.059	.059
.600	.400	.000	.000	.000	.000	.000
.000	.500	.250	.000	.000	.250	.000
.400	.200	.150	.000	.000	.050	.200

June 10 - June 23

.838	.064	.024	.014	.027	.010	.024
.510	.184	.061	.041	.041	.041	.122
.357	.286	.071	.000	.000	.143	.143
.333	.222	.000	.111	.111	.000	.222
.636	.091	.000	.091	.091	.000	.091
.250	.625	.000	.000	.000	.000	.125
.632	.211	.105	.000	.000	.053	.000

TABLE XXVI (continued)

PRECIPITATION TRANSITION PROBABILITIES
FOREST GROVE, OREGON

June 24 - July 7

.871	.072	.013	.016	.006	.006	.016
.564	.231	.077	.026	.000	.026	.077
.538	.154	.154	.000	.077	.000	.077
.375	.000	.250	.125	.000	.125	.125
.500	.167	.000	.167	.000	.000	.167
.143	.143	.143	.143	.143	.143	.143
.533	.267	.067	.000	.000	.133	.000

July 8 - July 21

.948	.027	.008	.003	.003	.000	.011
.600	.200	.000	.150	.000	.000	.050
.750	.250	.000	.000	.000	.000	.000
.857	.000	.143	.000	.000	.000	.000
.000	.000	.000	1.000	.000	.000	.000
.000	.000	.000	.000	.000	.000	.000
.667	.333	.000	.000	.000	.000	.000

July 22 - Aug 4

.955	.021	.013	.008	.000	.000	.003
.692	.154	.000	.000	.000	.077	.077
.800	.200	.000	.000	.000	.000	.000
.333	.333	.000	.000	.333	.000	.000
1.000	.000	.000	.000	.000	.000	.000
.500	.000	.000	.000	.000	.500	.000
.000	1.000	.000	.000	.000	.000	.000

Aug 5 - Aug 18

.931	.030	.008	.003	.011	.006	.011
.412	.235	.118	.000	.118	.118	.000
.333	.167	.000	.167	.167	.000	.167
.000	.000	.500	.000	.000	.000	.500
.500	.000	.125	.000	.125	.000	.250
.667	.333	.000	.000	.000	.000	.000
.444	.222	.111	.000	.111	.000	.111

TABLE XXVI (continued)

PRECIPITATION TRANSITION PROBABILITIES
FOREST GROVE, OREGON

Aug 19 - Sept 1

.862	.067	.016	.006	.003	.006	.038
.667	.179	.026	.000	.026	.026	.077
.500	.167	.083	.000	.167	.000	.083
.250	.500	.000	.000	.000	.000	.250
.667	.000	.000	.167	.000	.000	.167
.143	.000	.000	.000	.143	.286	.429
.346	.154	.154	.038	.000	.038	.269

Sept 2 - Sept 15

.863	.056	.022	.006	.009	.003	.041
.423	.231	.077	.038	.115	.038	.077
.588	.176	.059	.059	.059	.059	.000
.400	.200	.200	.000	.000	.200	.000
.500	.125	.125	.000	.000	.000	.250
.600	.000	.000	.200	.000	.000	.200
.280	.200	.160	.000	.040	.040	.280

Sept 16 - Sept 30

.870	.055	.020	.010	.010	.003	.031
.548	.214	.119	.024	.000	.024	.071
.500	.143	.000	.000	.000	.000	.357
.333	.000	.167	.000	.000	.000	.500
.444	.000	.000	.000	.111	.222	.222
.000	.250	.000	.250	.000	.000	.500
.189	.162	.081	.027	.135	.027	.378
.412	.176	.059	.176	.059	.059	.059

TABLE XXVII

STREAMFLOW STATISTICS
MAY - SEPTEMBER

Tualatin River near Gaston

DATE	MEAN (CFS)	STANDARD DEVIAITON	SKEW
May 1 - May 14	105.8	53.1	2.42
May 15 - May 28	76.8	44.9	3.03
May 29 - June 11	53.8	33.7	3.70
June 12 - June 25	37.5	18.8	2.37
June 26 - July 9	26.4	10.9	1.49
July 10 - July 23	20.1	7.7	1.21
July 24 - Aug. 6	16.2	6.9	0.90
Aug. 6 - Aug. 19	17.7	8.7	1.55
Aug. 19 - Sept. 2	21.3	7.9	1.09
Sept. 3 - Sept. 17	21.0	16.1	4.24
Sept. 18 - Sept. 30	22.8	14.7	-0.22

LOG TRANSFORMED FLOW

DATE	MEAN	STANDARD DEVIAITON	SKEW
May 1 - May 14	4.57	.397	0.88
May 15 - May 28	4.23	.430	1.09
May 29 - June 11	3.88	.424	1.32
June 12 - June 25	3.53	.386	1.16
June 26 - July 9	3.20	.377	0.34
July 10 - July 23	2.93	.358	0.25
July 24 - Aug. 6	2.70	.416	0.01
Aug. 6 - Aug. 19	2.77	.448	0.23
Aug. 19 - Sept. 2	2.99	.353	0.16
Sept. 3 - Sept. 17	2.90	.489	1.27
Sept. 18 - Sept. 30	2.96	.567	-0.38

CORRELATION COEFFICIENTS OF LOG TRANSFORMED DATA

LAG					
1	2	3	4	5	6
.8987	.7918	.7053	.6464	.6062	.5694

TABLE XXVII (continued)

STREAMFLOW STATISTICS
MAY - SEPTEMBER

Gales Creek

DATE	MEAN (CFS)	STANDARD DEVIAITON	SKEW
May 1 - May 14	116.7	63.0	2.71
May 15 - May 28	90.1	80.3	6.42
May 29 - June 11	56.8	26.0	3.15
June 12 - June 25	39.5	16.8	1.98
June 26 - July 9	27.4	10.5	0.55
July 10 - July 23	17.8	8.8	0.49
July 24 - Aug. 6	11.1	5.2	1.09
Aug. 6 - Aug. 19	10.6	10.2	8.48
Aug. 19 - Sept. 2	13.0	8.8	3.03
Sept. 3 - Sept. 17	11.8	9.9	3.80
Sept. 17 - Sept. 30	17.7	14.9	-0.28

LOG TRANSFORMED FLOW

DATE	MEAN	STANDARD DEVIAITON	SKEW
May 1 - May 14	4.66	.422	0.68
May 15 - May 28	4.34	.487	1.26
May 29 - June 11	3.96	.357	0.86
June 12 - June 25	3.61	.356	0.78
June 26 - July 9	3.23	.405	-0.40
July 10 - July 23	2.74	.554	-0.46
July 24 - Aug. 6	2.31	.437	0.29
Aug. 6 - Aug. 19	2.19	.524	0.71
Aug. 19 - Sept. 2	2.40	.567	0.01
Sept. 3 - Sept. 17	2.28	.549	1.05
Sept. 18 - Sept. 30	2.59	.732	-0.58

CORRELATION COEFFICIENTS OF LOG TRANSFORMED DATA

LAG					
1	2	3	4	5	6
.8856	.7862	.7032	.6430	.5953	.5578

TABLE XXVII (continued)

STREAMFLOW STATISTICS
MAY - SEPTEMBER

Dairy Creek

DATE	MEAN (CFS)	STANDARD DEVIAITON	SKEW
May 1 - May 14	160.8	72.0	1.32
May 15 - May 28	97.4	32.2	0.05
May 29 - June 11	61.3	21.0	0.16
June 12 - June 25	36.9	10.2	0.71
June 26 - July 9	32.0	23.0	5.59
July 10 - July 23	19.2	13.0	0.96
July 24 - Aug. 6	9.8	3.9	-0.15
Aug. 6 - Aug. 19	13.0	9.7	1.35
Aug. 19 - Sept. 2	16.5	8.2	0.12
Sept. 3 - Sept. 17	28.5	12.6	7.18
Sept. 18 - Sept. 30	16.3	10.5	-0.34

LOG TRANSFORMED FLOW

DATE	MEAN	STANDARD DEVIAITON	SKEW
May 1 - May 14	4.99	.406	0.40
May 15 - May 28	4.52	.366	-0.63
May 29 - June 11	4.05	.367	-0.33
June 12 - June 25	3.57	.269	0.11
June 26 - July 9	3.35	.434	0.85
July 10 - July 23	2.70	.799	-0.97
July 24 - Aug. 6	2.16	.578	-1.87
Aug. 6 - Aug. 19	2.27	.831	-0.51
Aug. 19 - Sept. 2	2.65	.602	-0.67
Sept. 3 - Sept. 17	2.45	.779	3.22
Sept. 18 - Sept. 30	2.63	.541	-1.30

CORRELATION COEFFICIENTS OF LOG TRANSFORMED DATA

LAG					
1	2	3	4	5	6
.7698	.6560	.5803	.5080	.4589	.4364

TABLE XXVII (continued)

STREAMFLOW STATISTICS
MAY - SEPTEMBER

McKay Creek

DATE	MEAN (CFS)	STANDARD DEVIAITON	SKEW
May 1 - May 14	47.5	25.7	1.65
May 15 - May 28	25.5	5.5	0.72
May 29 - June 11	16.5	4.2	0.75
June 12 - June 25	8.4	2.2	0.20
June 26 - July 9	6.8	2.0	0.12
July 10 - July 23	5.7	4.1	1.29
July 24 - Aug. 6	2.1	1.2	0.62
Aug. 6 - Aug. 19	2.9	3.7	2.13
Aug. 19 - Sept. 2	3.9	2.5	0.38
Sept. 3 - Sept. 17	3.0	2.0	0.61
Sept. 18 - Sept. 30	2.7	1.7	2.41

LOG TRANSFORMED FLOW

DATE	MEAN	STANDARD DEVIAITON	SKEW
May 1 - May 14	3.75	.441	0.96
May 15 - May 28	3.22	.209	0.37
May 29 - June 11	2.77	.244	0.38
June 12 - June 25	2.09	.274	-0.43
June 26 - July 9	1.88	.304	-0.40
July 10 - July 23	1.50	.719	-0.17
July 24 - Aug. 6	0.51	.752	-0.81
Aug. 6 - Aug. 19	0.46	1.07	0.39
Aug. 19 - Sept. 2	1.10	.788	-0.58
Sept. 3 - Sept. 17	0.84	.825	-0.54
Sept. 18 - Sept. 30	0.74	.759	0.41

CORRELATION COEFFICIENTS OF LOG TRANSFORMED DATA

LAG					
1	2	3	4	5	6
.8138	.6461	.5340	.4480	.3756	.3199

TABLE XXVII (continued)

STREAMFLOW STATISTICS
MAY - SEPTEMBER

Rock Creek

DATE	MEAN (CFS)	STANDARD DEVIAITON	SKEW
May 1 - May 14	122.6	105.2	2.80
May 15 - May 28	94.0	53.9	0.11
May 29 - June 11	53.8	33.5	0.25
June 12 - June 25	31.8	16.3	0.56
June 26 - July 9	25.8	27.9	1.27
July 10 - July 23	36.7	49.9	1.40
July 24 - Aug. 6	0.3	1.5	4.91
Aug. 6 - Aug. 19	0.6	2.8	4.63
Aug. 19 - Sept. 2	10.8	12.6	1.93
Sept. 3 - Sept. 17	16.3	10.6	0.20
Sept. 18 - Sept. 30	42.3	46.3	-0.19

LOG TRANSFORMED FLOW

DATE	MEAN	STANDARD DEVIAITON	SKEW
May 1 - May 14	4.35	1.583	-3.62
May 15 - May 28	4.29	.837	-1.15
May 29 - June 11	3.74	.783	-0.48
June 12 - June 25	3.31	.583	-0.67
June 26 - July 9	2.63	1.243	-0.32
July 10 - July 23	0.56	3.645	-0.04
July 24 - Aug. 6	-2.81	.965	4.91
Aug. 6 - Aug. 19	-2.64	1.296	3.42
Aug. 19 - Sept. 2	0.90	2.587	-0.75
Sept. 3 - Sept. 17	2.38	1.308	-2.55
Sept. 18 - Sept. 30	3.09	1.531	-0.04

CORRELATION COEFFICIENTS OF LOG TRANSFORMED DATA

LAG

1	2	3	4	5	6
.5233	.3604	.2420	.1731	.1130	.0859

TABLE XXVIII

ERROR COVARIANCE MATRICES
FOR SYSTEM FORECAST

3 Day Lead Time

0.000	0.000	0.000	0.000	0.000	0.000	0.000	0.000
0.000	47.214	40.319	25.074	14.001	6.166	-0.443	-1.477
0.000	40.319	35.053	23.191	14.230	7.056	1.411	0.016
0.000	25.074	23.191	32.638	22.774	13.079	6.723	4.210
0.000	14.001	14.230	22.774	57.547	30.947	11.634	5.427
0.000	6.166	7.056	13.079	30.947	19.911	14.119	9.651
0.000	-0.443	1.411	6.723	11.634	14.119	21.450	17.855
0.000	-1.477	0.016	4.210	5.427	9.651	17.855	16.513

4 Day Lead Time

0.000	0.000	0.000	0.000	0.000	0.000	0.000	0.000
0.000	66.628	54.415	28.964	12.693	4.077	-3.509	-2.912
0.000	54.415	46.081	27.984	15.298	6.722	-0.377	-1.228
0.000	28.964	27.984	52.661	36.024	19.913	8.387	3.903
0.000	12.693	15.298	36.024	74.445	38.341	11.415	4.820
0.000	4.077	6.722	19.913	38.341	25.652	19.323	12.451
0.000	-3.509	-0.377	8.387	11.415	19.323	33.053	25.468
0.000	-2.912	-1.228	3.903	4.820	12.451	25.468	23.401

TABLE XXVIII (continued)

ERROR COVARIANCE MATRICES
FOR SYSTEM FORECAST

5 Day Lead Time

0.000	0.000	0.000	0.000	0.000	0.000	0.000	0.000
0.000	82.623	64.605	29.240	9.562	1.837	-4.787	-2.448
0.000	64.605	53.781	30.796	15.447	6.165	-1.665	-1.902
0.000	29.240	30.796	69.543	44.151	21.998	4.192	-0.957
0.000	9.562	15.447	44.151	84.841	42.164	9.789	3.603
0.000	1.837	6.165	21.998	42.164	29.485	23.448	13.913
0.000	-4.787	-1.665	4.192	9.789	23.448	43.151	31.121
0.000	-2.448	-1.902	-0.957	3.603	13.913	31.121	29.739

6 Day Lead Time

0.139	0.000	0.128	0.103	0.080	0.051	0.035	0.025
0.000	95.709	71.978	28.002	6.780	0.604	-4.242	-0.995
0.128	71.978	59.738	33.424	15.960	5.962	-2.510	-2.231
0.103	28.002	33.424	84.606	49.640	22.505	-0.129	-3.968
0.080	6.780	15.960	49.640	92.967	45.538	9.379	3.178
0.051	0.604	5.962	22.505	45.538	33.028	27.079	14.501
0.035	-4.242	-2.510	-0.129	9.379	27.079	50.637	34.304
0.025	-0.995	-2.231	-3.968	3.178	14.501	34.304	34.586

TABLE XXVIII (continued)

ERROR COVARIANCE MATRICES
FOR SYSTEM FORECAST

7 Day Lead Time

0.145	0.000	0.121	0.065	0.023	-0.001	-0.030	-0.033
0.000	106.835	77.760	26.649	5.127	0.339	-2.972	0.223
0.121	77.760	64.930	36.393	16.703	5.799	-3.450	-2.528
0.065	26.649	36.393	98.098	53.353	22.405	-3.463	-5.085
0.023	5.127	16.703	53.353	100.003	48.730	9.332	2.409
-0.001	0.339	5.799	22.405	48.730	36.130	29.809	14.372
-0.030	-2.972	-3.450	-3.463	9.332	29.809	56.014	36.566
-0.033	0.223	-2.528	-5.085	2.409	14.372	36.566	39.257